ANALYSIS OF MAMMALIAN TUMOR VASCULARIZATION IN THE DEVELOPMENT OF A THERAPY TO PREVENT METASTASIS

by
Anthony V. D'Amico

B.S., Physics, Massachusetts Institute of Technology
(1983)

B.S., Nuclear Engineering, Massachusetts Institute of Technology
(1984)

M.S., Nuclear Engineering, Massachusetts Institute of Technology
(1984)

SUBMITTED TO THE DEPARTMENT OF NUCLEAR
ENGINEERING IN PARTIAL FULFILLMENT OF
THE REQUIREMENTS FOR THE DEGREE OF

DOCTOR OF PHILOSOPHY

at the

MASSACHUSETTS INSTITUTE OF TECHNOLOGY

April 29, 1986

Signature of Author_____
Department of Nuclear Engineering

Certified by_____
Alan C. Nelson
Thesis Supervisor

Accepted by_____
Allan F. Henry
Nuclear Engineering Department
Chairman on Graduate Students

ANALYSIS OF MAMMALIAN TUMOR VASCULARIZATION IN THE DEVELOPMENT OF A THERAPY TO PREVENT METASTASIS

by

Anthony V. D'Amico
Submitted to the Department of Nuclear Engineering on April 29, 1986
in partial fufillment of the requirements for the degree of
Doctor of Philosophy

ABSTRACT

Using syngeneic Wistar-Lewis rats as the experimental subject, the spontaneously arising renal adenocarcinoma of the clear cell type is implanted under the renal capsule of the rat's left kidney while the right kidney is used as a control. In one week intervals from three weeks to a maximum of six weeks post implantation, a polymer casting procedure(Shah, 1983; Babayan, Nelson, D'Amico, 1985) is employed to create a plastic replica of the kidney-tumor microvasculature. The plastic cast is analyzed to test the hypothesis that if a tumor engulfs some fraction of its own vasculature as it grows, it leaves beneath its expanding surface a fraction of the vasculature which may become open ended. This open vessel system could provide a mechanical pathway for tumor cells detached from the primary growth to travel into the main circulatory system where they may be potentially involved in metastases. An understanding of this pathway could help explain how the proliferation of secondary growths at the site of the target tissue can be initiated in the metastatic process.

In this investigation the use of thrombin as both a tumor growth inhibitor and anti-metastatic agent is studied using two transplantable renal tumor systems, adenocarcinoma(White, 1980) and rhabdomyosarcoma(Barendsen, 1970) in the syngeneic Wistar-Lewis and Wag-Rij rats respectively. From studies of tumor implantation on renal systems (Babayan, Nelson;1984) it is shown that renal adenocarcinoma metastasizes to the lung at eight weeks post implantation leading to animal death in ten weeks due to the lethal effects of the lung metastases. Likewise, the rhabdomyosarcoma metastasizes to the lung at seven weeks post implantation leading to a similiar lethality in the animal.

The administration of one bolus injection of thrombin to the tumor necrotic region at six weeks post-implantation(pre-metastatic) prolongs the time to metastasis to approximately twenty weeks post-implantation(or roughly double the life expectancy following tumor

implantation) depending on the tumor diameter at the time the thrombin is delivered. In addition, the growth rate of the primary tumor is considerably decreased probably due to vascular thrombosis of the tumor vasculature leading to increased ischemia and subsequent tumor necrosis.

The results of the morphological examination and the success of the thrombin therapy provide evidence for the existence of a radially directed open vessel pathway in the metastatic process. From the results of the students t-test on the morphological data one can assert on a statistical basis with at least 95%($p < 0.05$) certainity that inward directed radial tumor vasculature exists. Two classes of these inward radial tumor vessels are found: Class 1 consists of vessels that are not active mitotically but are open-ended; Class 2 consists of vessels that are active mitotically (i.e. growing) but are closed-ended; indicating the growth of new tumor vasculature. Class 1 tumor vessels may provide the entrance into which thrombin can permeate and fill the entire tumor parenchyma resulting in both tumor toxic and anti-metastatic effects.

Thesis Supervisor: Professor Alan C. Nelson

Title: Associate Professor of Nuclear Engineering and the Whitaker College of Health, Sciences, Technology and Management

ACKNOWLEDGEMENTS

The author acknowledges with sincere thanks the compliance and assistance given to him by his Thesis Supervisor, Professor Alan C. Nelson. His role in the creation of this work was both as a friend and a counselor. His unselfish efforts and understanding nature enabled the author to continue the work during times of academic, physical, and/or social trials.

Also, the author wishes to express his gratitude to Dieu Thu Vo who spent many hours assisting the author with many aspects of this work including tumor implantation, thrombin therapy, vascular polymer casting and histological methods.

A deep thanks is extended to Dr. Richard Babayan for offering both his time to teach the author the renal tumor implantation technique and providing the author with donor rats infected with renal adenocarcinoma. Also, the author wishes to recognize both Dr. Christian E. Newcomber and Dr. Pamela A. Phillips at M.I.T.'s Division of Comparative Medicine for teaching the author the proper surgical method needed to create a closed vascular system on which the polymer casting method was employed.

Finally, a very great appreciation and respect is expressed to the author's parents, Mr. and Mrs. Victor and Annette D'Amico, who have

provided him with the foundation from which all his achievements have been made possible.

TABLE OF CONTENTS

LIST OF FIGURES

LIST OF TABLES

1. INTRODUCTION and BACKGROUND

1.1 Background

For the most part, cancer starts as a localized proliferation of cells arising from a single cell within a region of transformed cells. As cell proliferation at the origin continues, there is often an increase in the volume of the local proliferating cell mass and a consequent rise in local tissue pressures. Microscopically, and often visually with pigmented tumors clinically, one can observe that around the central mass of proliferating cells, there are extensions of these cells that develop in the cracks and crevices of the surrounding tissue. They dissect along the tissue planes, may erode into vascular or lymphatic channels and may extend for considerable distances while maintaining continuity with the initial cell mass. Often, however, such extensions are recognized only by the secondary effects, such as fibrosis, produced by the migrating cells. Uniformity in extension generally does not exist, since the boundaries are quite irregular in both lateral and depth penetration with superficial cancers, and in size, shape, and extent with central growths(Poste, 1977).

The tumor cell extensions at any given time may be more widespread than clinical examination can determine, and thus the surgeon is faced with the possibility of incomplete excision. The initial tumor together

with the probable area of invasion, must be excised. Removal of too much tissue generally increases morbidity; yet removal of too little may lead to local recurrence, which may be increasingly difficult to treat(Kleinerman, 1974).

1.2 Tumor Formation and Angiogenesis

Cancer cells are motile, have decreased mutual adhesiveness, reduced contact inhibition, and can elaborate through tissues. Also, they can secrete a compound called "tumor angiogenesis factor" (TAF) which has been recently purified by Folkman(Folkman, 1985). Attempts to uncover the mechanisms of angiogenesis have revealed the following:

(a) Angiogenesis itself is a multi-stage process in some ways analogous to blood coagulation and

(b) the induction of neovascularization is not unique to tumors but is associated with a variety of physiological and pathological processes such as wound healing, maturation of the corpus luteum, chronic inflammation, and delayed hypersensitivity.

In physiologic situations, as for example development of the corpus luteum, angiogenesis seems to be necessary for completion of the process and subsides or is turned off once the process is completed. In certain pathologic states that are not malignant, angiogenesis is abnormally prolonged although self-limiting. Examples are pyogenic granuloma, keloid formation, or retrolental fibroplasia. By contrast, angiogenesis in malignancy is not self-limiting. Once tumor-induced angiogenesis is turned on, it continues indefinitely until all of the tumor is eradicated or the host dies(Folkman, 1976).

The actual process by which new capillaries grow in response to a tumor does, however, appear to be remarkably similiar to the capillary proliferation associated with non-malignant angiogenesis. Common to all forms of angiogenesis is a general pattern of response by the capillary endothelial cell. The release of TAF has been shown to cause capillary endothelial cells to grow in a manner that directs capillary growth towards the tumor(Folkman, 1975). Continuous vascularization of the tumor increases the supply of nutrients available for tumor growth. Cancer cells can migrate, lose connection with the parent growth, and enter the bloodstream. Even though the mere presence of malignant cells in the blood is not diagnostic for metastasis(Salsbury, 1975), the fact that cancer cells do circulate in the bloodstream, specifically during surgery, is thought to contribute to the likelihood of metastasis.

Also, it is important to note that past experiments(Folkman, Langer, etc..) imply that whatever the angiogeneic stimulus, it must be continually present to maintain newly formed vessels. Removal of an angiogenic stimulus is followed in one to two days by changes in the endothelial cells located at the distal tips or loops of a new capillary vessel. Mitochondria swell and some cells become thin and develop fenestrations that may not be seen in healthy, non-regressing vessels. Endothelial cells seperate, permitting escape of erythrocytes. Platlets then adhere to the degraded endothelium. These platlets are frequently degranulated and associated with strands of polymerized fibrin. Platlet

sticking is followed by stasis and these two events appear to be the trademark of capillary regression.

Preliminary experimental evidence suggests that certain angiogenesis inhibitors provoke similiar events. Little is known about why an endothelial cell in a new capillary suddenly loses its ability to repel platlets once a neovascular stimulus is removed; whereas, the endothelial cells of more established vessels do not.

Once stasis occurs, endothelial cells degenerate. Macrophages move in perivascular tissue to surround the degenerating capillaries and ingest cell debris. Stasis and phagocytosis proceed in a retrograde manner from the tip of the capillary. After six to ten weeks all vessels are replaced by lipid filled macrophages(termed foam cells for their appearence under light microscope) and a few fibroblasts. Only the thin white threads of the largest primary vessels mark the location of the original capillary plexus.

1.3 Theories of Metastasis

Metastasis is the spreading of tumor colonies from malignant cells that detach themselves from the primary tumor and travel through the body, usually but not exclusively, via the vascular system, and often to distant sites. The development of metastasis involves a complex sequence of interdependent events best conceptualized as a stairway depicted in figure 1 where each step must be successfully surmounted to eventually produce a secondary implant.

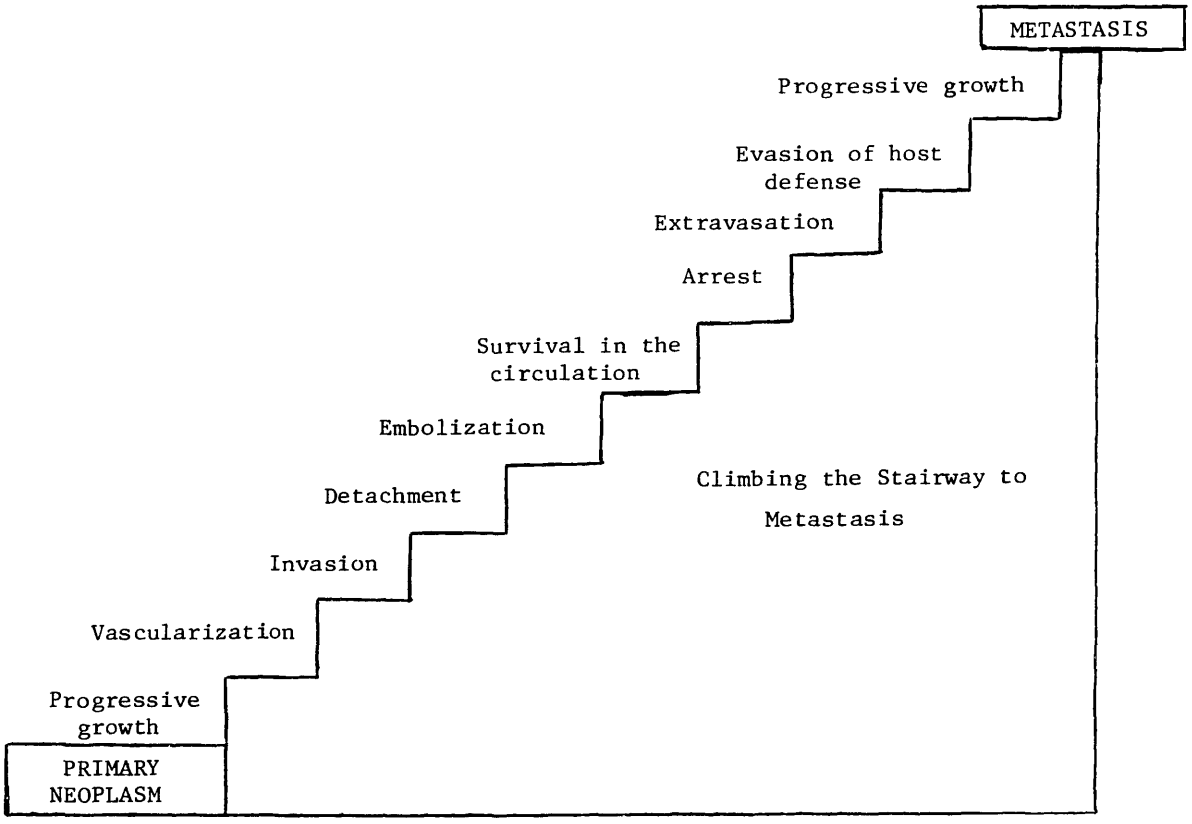

Figure 1: Sequential development of processes leading to metastasis.

The initial steps in this sequence were discussed in the previous section. Starting at the invasion level the detached cells from a primary carcinoma may first enter open lymphatics, and then thin walled veins, or less commonly thicker walled arteries. Sarcomas tend to enter blood vessels earlier unlike carcinomas that enter lymphatics first. From the lymphatics the cells spread to the regional lymph nodes, where the tumor may be arrested. If not, growth in nodes and furthur dissemination occurs eventually reaching the circulatory system. A tumor's growth may also block a lyphatic duct leading to a reverse spread. In general, once the cells have invaded the vascular or lymphatic channels they may either grow at the site of penetration or, because of their loss of cohesiveness, be swept away as individual cells or small embolic clumps. In this exposed situation they are vulnerable to humoral or cell-mediated immune responses and to nonimmune defenses such as destruction by activated macrophages or natural killer(NK) cells. Conversely they may become coated with polymerized fibrin(Dvorak, H.F.,1979;Chew, E.C. and Wallace, A.C., 1976) or platlet aggregates, both of which could enhance survival of intravasular cancer cells, and therfore the formation of metastases. The cells that survive must then arrest in the capillary beds of distant organs either by adherence to endothelial cells or attachment to vascular basement membrane exposed by endothelial cell retraction(Kramer, R.H. and Nicolson, G.L.,1979). The arrest of circulating tumor cells is not a haphazard process, rather extravasation of cells at sites of arrest presumably involves the same

ill-defined influences that determine the invasiveness of primary neoplasms. Thereafter the metastasis must avoid the host immune response, develop its own vascularization, and in this way, unfortunately, produce a secondary implant that often presages the beginning of the end for the patient.

1.4 Tumor Patholgy and Nomenclature

All tumors benign and malignant, have two basic components:

(1) proliferating neoplastic cells that constitute their parenchyma and
(2) supportive stroma made up of connective tissue, blood vessels, and possibly lymphatics.

Although parenchymal cells represent the "cutting edge" of neoplasms and so determine their nature, the growth and evolution of neoplasms are critically dependent on their stroma. An adequate stromal blood supply is requisite and the stromal connective tissue provides the framework for the parenchyma. In some tumors the stromal support is scant, and so the neoplasm is soft and fleshy. Sometimes the parenchymal cells stimulate the formation of an abundant collagenous stroma(referred to as desmoplasia). Such tumors as, for example, some cancers of the female breast are stony hard or scirrhous.

The nomenclature of tumors is, however, based on the parenchymal component. The suffix "oma" denotes a benign neoplasm. Benign mesenchymal tumors(those arising in muscle, bones, tendon, cartilage, fat, vessels, and lymphoid and fibrous tissue) are classified histogenetically according to parenchymal cell type.

Malignant tumor nomenclature essentially follows the same schema used for benign neoplasms with certain additions. Cancers arising in mesenchymal tissue are called sarcomas because they usually have very little connective tissue stroma and so are fleshy(Greek "sarc-" = fleshy): e.g. rhabdomyosarcoma for a cancer arising in straited muscle. Malignant neoplasms of epithelial cell origin, derived from any of the three germ layers, are called carcinoma. One with a glandular growth pattern microscopically is termed and adenocarcinoma, and one producing recognizable squamous cells arising in any of the stratified squamous epithelia of the body would be termed a squamous cell carcinoma. Finally, it is common practice to specify, when possible, the organ of origin, e.g. a renal cell adenocarcinoma for a glandular epithelial neoplasm from the kidney.

Nearly all benign tumors grow as localized expansile masses enclosed within a fibrous capsule. They remain localized to their site of origin and cannot disseminate throughout the body. The capsule comprises an enclosing fibrous membrane, in part derived from the fibrous stroma of the surrounding normal tissue and in part elaborated by the tumor. Such encapslation tends to contain the benign neoplasm as a discrete readily palpable, and easily movable mass that can be surgically enucleated.

Cancers are almost never encapsulated and are characterized by infiltrative, erosive growth that extends crablike feet into adjacent

tissues. Slowly expanding malignant tumors may develop an apparently enclosing fibrous membrane and may push along a broad front into adjacent normal structures. However, histologic examination will almost always disclose tiny pseudopods indicative of penetrating spread.

Most cancers are obviously invasive and can be expected to penetrate the wall of the colon or the uterus, for example, or fungate through the surface of the skin. They recognize no normal anatomic boundaries and often permeate lymphatics, blood vessels and perineural spaces as previously noted. Such invasiveness makes their surgical resection exceedingly difficult and generally requires removal of a considerable margin of apparently normal tissues about the infiltrative neoplasm; this is referred to as radical surgery. In fact, next to the development of metastases, invasiveness is the most reliable feature that differentiates malignant and benign neoplasms.

1.5 A Vascular Metastatic Pathway

In this work the existence of open-ended tumor vessels in the tumor hypoxic region is established. It is postulated that one pathway through which malignant cells could enter the circulation is through open-ended tumor vessels. These open vessels are thought tc be created by the degradative action of active lysosmal enzymes diffusing outward from the tumor necrotic region towards the endothelium of closed tumor vessels (Weiss, 1978; Turner,1980). A polymer casting method and scanning electron microscopy are used to investigate tumor microvasculature (Shah, 1983; Babayan,1984; Nelson, 1984) and an inverse square correlation is established between the time to metastasis and the number of open-ended tumor vessels. This correlation provides substantial evidence that the open tumor vessel system provides a pathway for metastasis.

1.6 Models for Tumor Vascular Morphology

The current view of the morphology of tumor vasculature(Peterson, 1979) is that it is located only on the periphery of the expanding tumor and forms a closed vascular network(i.e no open-ended vessels). In the present investigation the hypothesis is that if a tumor engulfs any fraction of its own vasculature as it grows, then it may leave beneath its expanding surface vasculature which may become open-ended. This open system provides a mechanical pathway for the migration of tumor cells into the main circulatory system where they may be subsequently sequestered in the vascular endothelium of the target tissue. This pathway could explain how the secondary growth at the site of the target tissue may be initiated.

If the tumor vasculature is exclusively peripheral then expansion of the tumor peripherally and the concurrent expansion of the necrotic region internally would not result in open-ended vessels(Figure 2a). However if the peripheral vessels contain radially directed branches then internal expansion of the necrotic region could lead to vessel degradation(Figure 2b). Therefore, the first step in the establishment of open-ended tumor vessels is to establish that radial tumor vessels exist.

In this investigation the establishment of open-ended tumor vessels and its connected vascular network allows for the statement of the fol' ing hypothesis:

HYPOTHESIS

Open-ended inward directed radial capillaries in solid tumor could provide passage to the main circulatory system for cancer cells that have detached from the non-necrotic region of the tumor, thus providing a physical pathway mechanism for metastasis.

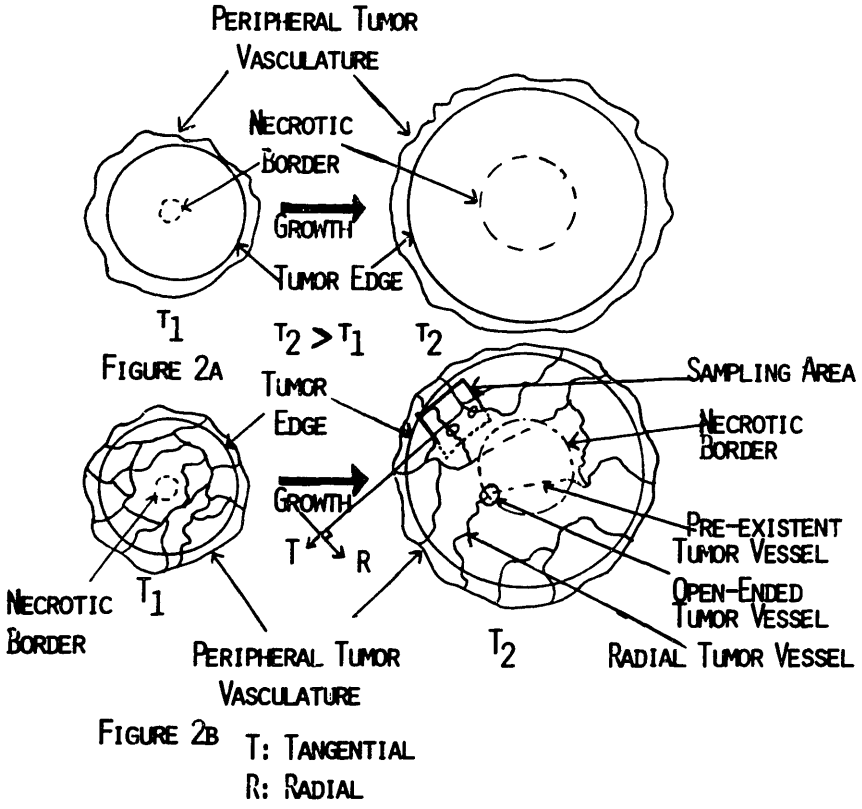

Figure 2a: Conventional model of tumor vessel growth.
2b: Proposed model of tumor vessel growth.

1.7 Thrombin As A Potential Chemotherapeutic Agent:

Thrombin, a direct acting coagulant, is a protein substance produced in mammals through a conversion reaction in which pro-thrombin is activated by tissue thromboplastin in the presence of calcium chloride. As a tumor therapy agent, thrombin may be useful in reducing tumor perfusion and blocking metastasis. More specifically, an injection of thrombin into the tumor necrotic region allows the coagulant to diffuse through the tumor mass and permeate the tumor vasculature(via the open-ended radial tumor vessels) to form thrombi. Thrombus formation serves two anti-tumor functions(D'Amico, 1986). First, thrombus formation restricts blood flow and concomitantly reduces tumor perfusion giving rise to tumor hypoxia, hypolycemia, and deficiencies in other blood borne compounds(e.g. vitamins, amino-acids, minerals). These deficiencies promote tumor necrosis. Second, thrombosis of the tumor vasculature reduces the possibilty of metastasis by sealing off the tumor vessel system from the rest of the organism's circulatory system.

Because the metastatic colonies are harder to detect than the original tumor and, moreover; are often impossible to treat successfully, metastasis can be considered clinically as the conclusive event in the natural history of cancer(Nicolson, 1979). Therefore, a therapy(such as the one described here) that has both anti-tumor and anti-metastatic effects could be effective in the long term control and eventual elimination of malignancies in patients.

2. EXPERIMENTAL METHODS

2.1 Tumor Vascular Studies:

In the first part of this work, tumor vascular studies are performed to enable the understanding of the three-dimensional morphology of tumor neovasculature. The methods involve the creation of a plastic cast replicas of the tumor vasculature which are examined under a scanning electron microscope.

2.1a Animal Surgery and Tumor Implantation

The spontaneously arising renal adenocarcinoma of the clear cell type is implanted in the renal capsule of the Wistar-Lewis rat's left kidney while the right is used as a control. The Wistar-Lewis rat is used as the test subject, because there is no immunological rejection when the adenocarcinoma tumor is implanted under the renal capsule(White, 1980). The tumor tissue was obtained from Dr. Richard Babayan at Boston City Hospital, Boston, Massachusetts.

Renal adenocarcinoma is found in this study and others(Babayan, Nelson; 1984) to have its primary metastatic site at the lung approximately eight weeks post-implantation in the renal capsule. Most rats die at about ten weeks post-implantation due to inadequate alveolar

surface area for blood gas exchange resulting from the presence of tumor on the pulmonary tissue. A small percentage(less than 2%) of the rats in this study lived long enough to sustain a secondary hepatic metastasis at 12 weeks post-implantation.

2.1b Polymer Casting of Tumors

In one week intervals from three weeks up to a maximum of six weeks post tumor implantation, a surgical procedure was performed on 15 rats(in each age group) to create a "closed vascular system" involving both of the rat's kidneys and the lower abdominal aorta and inferior vena cava(figure 3).

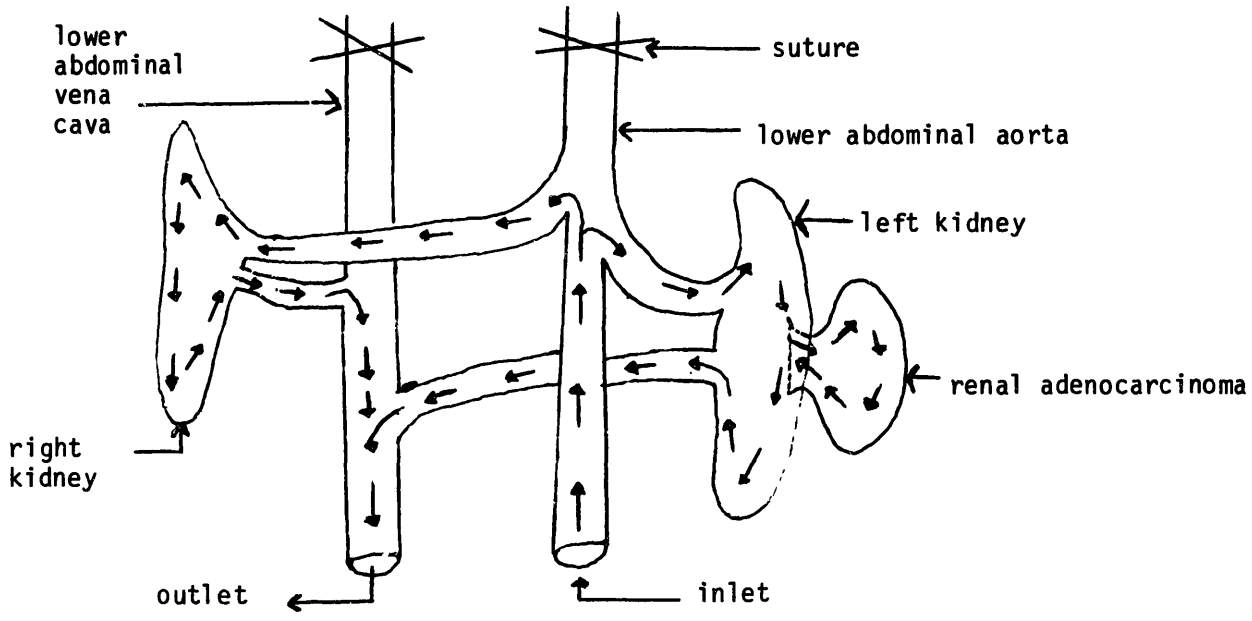

Figure 3: Closed vascular system used for the preparation of kidney-tumor system.

This system was catheterized through the lower abdominal aorta. The aorta serves as the inlet while the vena cava serves as the outlet for perfusion. We perfused with 50 ml of 0.85% heparnized saline in order to drain the blood from the vascular system and prevent thrombus formation. Then, 50 ml of 2.5% gluteraldehyde(ph=7.4, buffered with $NaH_2PO_4 \cdot H_2O$ and $NaH_2PO_4 \cdot 7H_2O$) is adminstered as a fixative. Perfusion with the fixative ensures that the vasculature will not collapse or rupture during polymer injection. Finally, the system is injected with a low viscosity methyl methacrylate polymer called Mercox(Ladd Research Industries, Inc., Burlington, VT). The polymer hardens within 15 minutes; the kidneys are surgically removed and digested in a preparation of 5.6 N potassium hydroxide(20% by weight) at room temperature until the biological tissue completely dissolves, leaving a plastic replica of the kidney-tumor microvasculature.

2.1c Scanning Electron Microscopy

The small(< 2 cm diameter) plastic casts are processed for SEM in the standard fashion of dehydration in graded ethanol, drying in a carbon dioxide critical point dryer, and mounting on aluminum stubs for gold sputter coating. The larger casts were air dyred before mounting. All specimens(15 from each age group) were studied under the scanning electron microscope(ISI DS-130) which is operated at 20 kV potential in the secondary electron model. During data collection several views of the specimens were obtained by using the tilt mechanism on the SEM. Viewing the specimen in several different planes allowed for a three dimensional visualization of the tumor vascular morphology.

2.2 Thrombin Therapy

Animal surgery, polymer corrosion casting method, scanning electron microscopy(SEM), and histology are used to investigate the effects of thrombin therapy on tumor microvasculature. Figure 4 is a flow chart of the various procedures performed on 104 Wistar-Lewis rats and 16 Wag-Rij rats used in this study.

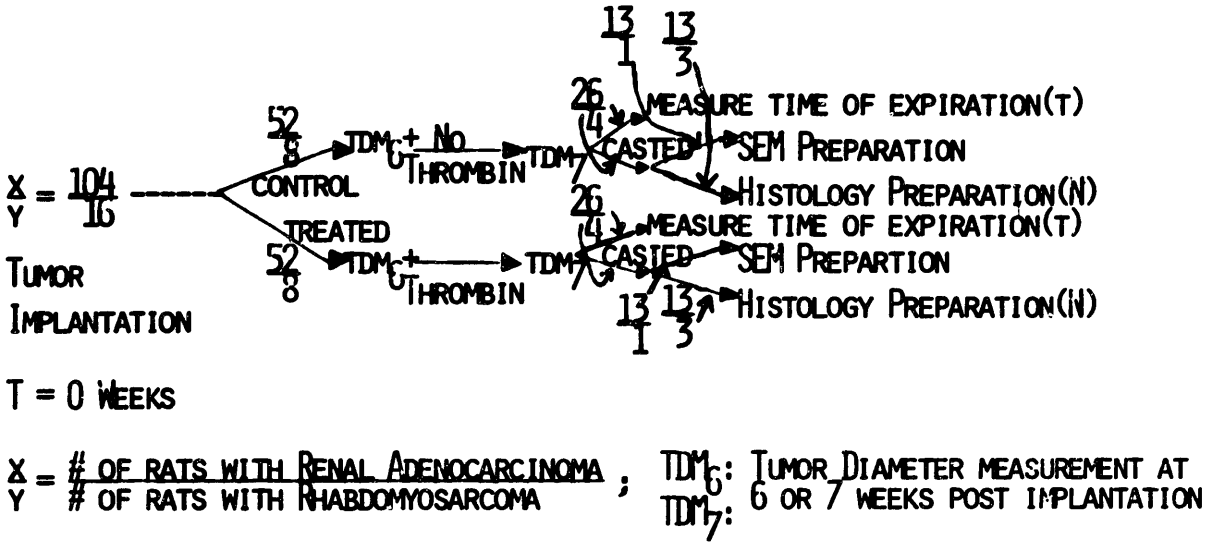

Figure 4: Flowchart of experimental methods.

The spontaneously arising renal adenocarcinoma and rhabdomyosarcoma are implanted under the left renal capsule of the Wistar-Lewis and Wag-Rig rats respectively while the right kidney in each is used as a control. A 1 mm^3 mass of adenocarcinoma tumor tissue is implanted beneath the Wistar-Lewis rat's left renal capsule where there appears to be no immunological rejection of the tumor mass(White, 1980). Similarly, the rhabdomyosarcoma tumor tissue was implanted under the Wag-Rij rat's renal capsule(Barendsen,Broerse; 1969,1970).

At six weeks post implantation the rat's left kidney-tumor complex is exposed and examined. The tumor diameter is measured(measurement is obtained by taking the square root of the product of the largest and smallest diameters) and then one half of these animals (52 Wistar-Lewis rats and 8 Wag-Rij rats) are returned to their cages untreated to serve as controls. The remaining half of the animals(52 Wistar-Lewis rats and 8 Wag-Rij rats) are given a single injection of thrombin into the center of the tumor necrotic region after which they are returned to their cages.

2.2a Thrombin Dose Calculation

The thrombin dose administered is a function of tumor radius and has been calculated(Appendix D). It is assumed that the injected dose of thrombin diffuses isotropically through tumor tissue and can be modeled as an instantaneous point source. Under these conditions the concentration of thrombin as a function of radius(r) and time(t) is given by equation 1.

$$C(r,t) = (U/8(\pi Dt)^{1.5})e^{(-r^2/4Dt)} \qquad (1)$$

where:

U: the number of units of thrombin delivered to the tumor necrotic region

D: 1.8 E-5 cm^2/sec [Thrombin diffusion coefficient]

Figure 5 shows a graph of the solution to equation (1). The therapeutic thrombin dose in this study is 2 units of thrombin(stock solution is 5000 U/ml) to clot 1 ml. of animal's blood in 15 seconds. From figure 5 one can note that at a time(t) equal to t_{max} the concentration of thrombin is at a maximum at the location, $r = (6Dt_{max})^{.5}$

from the point of thrombin injection. The time, t_{max} is of interest because by evaluating equation 1 at $t = t_{max}$ for a given tumor radius, r_{tumor} and using C-therapeutic = 2 units thrombin/ml blood for $C(r,t_{max})$, one can solve for the number of thrombin units, U needed such that at time $t = t_{max}$ the thrombin concentration $C(r=r_{tumor},t_{max})$ would have reached therapeutic levels throughout the entire tumor. The calculation of U is contained in Appendix D.

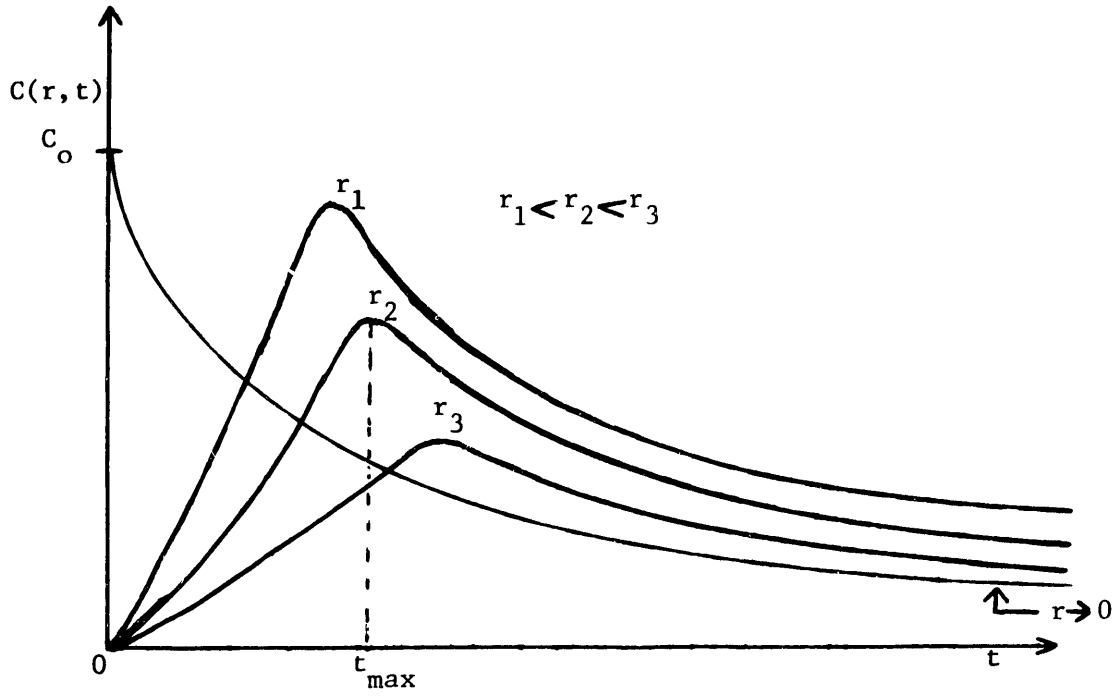

Figure 5: Concentration profile in time for varying tumor radii, note t_{max} is shown for $r=r_2$.

To calculate t_{max} one looks for the critical point in the C(r,t) function in the time domain as follows:

From $dC(r,t)/dt \,/= 0$ (2)

$t=t_{max}$

one finds:

$$t_{max} = r^2/6D \quad (3)$$

Table 1 gives the t_{max} and tumor radius, r_{tumor}, with the corresponding number of units of thrombin, U, required for therapy as determined from equation 1.

r_{tumor}(cm)	# Units of thrombin	t_{max}(hours)
0.5	50	0.64
1.0	400	2.60
1.5	1,348	5.80
2.0	3,194	10.3
2.5	6,239	16.1
3.0	10,781	23.2

Table 1: Summary of the proper thrombin dosage and time, t_{max} to achieve a maximum thrombin concentration at the tumor boundaries for tumors of varying radii.

2.2b Specialized Vascular Casting

After the rat kidney-tumor system is injected with the appropriate thrombin dose, half of the treated animals(26 Wistar-Lewis, 4 Wag-Rij) are maintained until death and their expiration date and cause of death are noted while the remaining animals(26 Wistar-Lewis, 4 Wag-Rij) are held one week and then undergo a vascular casting procedure and a tumor diameter measurement. As can be seen from the t_{max} times listed in Table 1, one week is ample time for the drug to have reached therapeutic levels in all tumor regions for the tumor specimens used in this study(i.e. $r_{tumor} < 6$ cm).

A specialized vascular casting procedure was performed on half of the thrombin treated animals (26 Wistar-Lewis, 4 Wag-Rij) involves surgical exposure of the rat's left kidney-tumor complex followed by a polymer injection of methyl methacrylate, Mercox (Ladd Research Industries, Inc., Burlington, Vt.) into the center of the tumor necrotic region. After injection under hand pressure(approx. 50 torr) the polymer is allowed to harden for thirty minutes. Approximately half of the casted specimens(13 Wistar-Lewis,3 Wag-Rij) are sectioned into 5 mm slices and stored in Sierra's fixative(Appendix A) in preparation for histological slide preparation(Appendix A).

The remaining casted specimens are prepared for SEM(13 Wistar-Lewis, 1 Wag-Rij). Preparation for SEM involves digestion of the kidney-tumor

casts in 20% by weight solution of potassium hydroxide(5.6 N), followed by dehyradation in graded ethanol, drying in a carbon-dioxide critical point dryer, and mounting on aluminium stubs prior to gold sputter coating. The specimens are studied under the SEM (ISI DS-130) which is operated at 20kV potential in the secondary electron mode.

For the untreated(control) animals(52 Wistar-Lewis, 8 Wag-Rij) the tumor diameters are measured at six weeks post implantation. Half of these animals(26 Wistar-Lewis, 4 Wag-Rij) are caged and are monitored as to the time and cause of death. The remaining animals(26 Wistar-Lewis, 4 Wag-Rij) undergo the specialized vascular casting procedure at seven week post implantation previously described. Finally, approximately half of the casted specimens (13 Wistar-Lewis, 1 Wag-Rij) are prepared for SEM examination; whereas the rest of the casted control specimens(13 Wistar-Lewis, 3 Wag-Rij) are processed for histological sectioning(Appendix A) and light microscope slide production(Appendix A).

The cause of death in all cases of both control and treated rats is pulmonary metastasis to both lungs leading to insufficient alveolar surface area for blood gas exchange(White, 1980). In all cases examined the fatal metastasis occured at two weeks $\pm$ one day prior to animal expiration and, as a result, the time to metastasis is given as the time to animal expiration minus two weeks($\pm$ one day).

2.2c Histological Preparation

The histological slide preparation(Appendix A) involves specimen dehydration in ethanol and chloroform, followed by infiltration and embedment in paraffin at 60°C. The embedded specimens are cut into ten micron thick slices, mounted on glass slides, and stained with hematoxylin and eosin. These slides are examined under a Zeiss 47 79 01 9901 light photomicroscope III.

3. RESULTS

The results of both the tumor vascular studies and thrombin therapy trials are presented. Open-ended radial vessels are established with at least 95% certainity and the efficacy of thrombin as an anti-metastatic agent is validated.

3.1 Testing of a New Model for Tumor Vascular Morphology

To show with adequate statistical certainty that radial tumor vessels exist, a student t-test is performed on the data collected from the kidney-tumor polymer cast specimens. Any capillary that points radially inward gets counted provided its angle with the tangent plane at the tumor surface is greater than 30 degrees(Figure 2b, Figure 7). This criterion was imposed to ensure that the vasculature was in fact pointing towards the tumor center and not lying along the tumor surface(i.e. peripheral).

3.1a Calculation of the Sample Area

In performing the student t-test a sample area size must be determined. A square area of 500 um x 500 um is adopted to ensure that within any square area of evaluation there could be at least one data point. The determination of the dimensions of the sample area was performed as follows: The average intercapillary distance for tumor systems examined in this study is 190 um(Peterson, 1979) . Using the intercapillary distance(ICD) one can construct a circle of capillaries around a central capillary such that all capillaries are at a distance of 190 um from one another(Figure 6a). If one inscribes a square within the circle which encloses only one capillary, this square area would represent the choice for which a value of unity would be obtained as the data point. Therefore by calculating the dimension of this inscribed square one can find the smallest allowable dimension of the sample area such that at least a value of unity could be obtained on any given counting trial. The length of the side(L) is given by equation 4 in terms of the ICD.

$$L = (2)\cdot^{5}ICD \qquad (4)$$

Evaluating equation 4 for the tabulated ICD gives a dimension L of 266 um. The method described represents the closest possible packing of

capillaries. In order to be certain that the largest possible sample size has been choosen to include one capillary, evaluation of the capillary packing shown in figure 6b should be analyzed since it represents the least dense close packing of capillaries. In this case the dimension of the sample area side is 2ICD or 380 um. In this study the conservative value of 500 um is choosen because the ICD reported is an average and may vary as much as $\pm$ 20 um depending upon the tumor and its size.

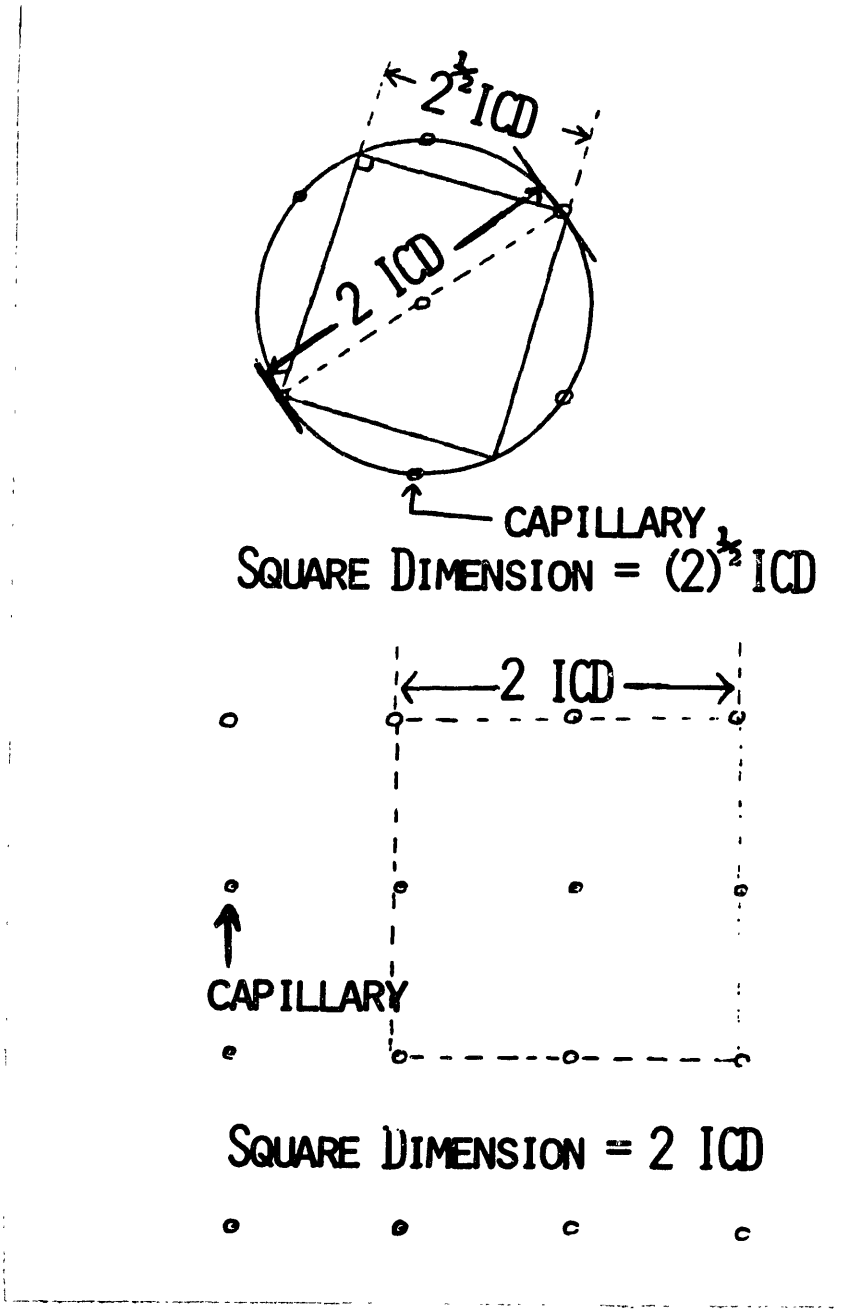

Figure 6a: Illustration of the calculation to determine the sample area dimensions(closest packing).

6b: Illustration of the calculation to determine sample area dimensions(least dense packing).

3.1b The Counting Experiment: Methods and Results

Each of forty different tumor specimens(10 from each age group) are measured as follows:

(1) For a given tumor age(i.e. 3, 4, 5, and 6 weeks) 500 um x 500 um squares of tumor surface vasculature are examined under SEM(magnification = 200X, approximately).

(2) For the fixed 2.5 E+5 um^2 area(box shown in figure 2b, figure 7) the number of radial tumor vessels satisfying the criterion stated above are counted and this number serves as a data point. One hundred sample areas are chosen randomly for each specimen to avoid biasing the data.

(3) For a given tumor specimen as many as three different angles of view are chosen for each observation in order to establish the angular arrangement of tumor vascular morphology(See figure 7). These three views were obtained by tilting the SEM specimen stage at angles varying between $\pm$ 15 degrees.

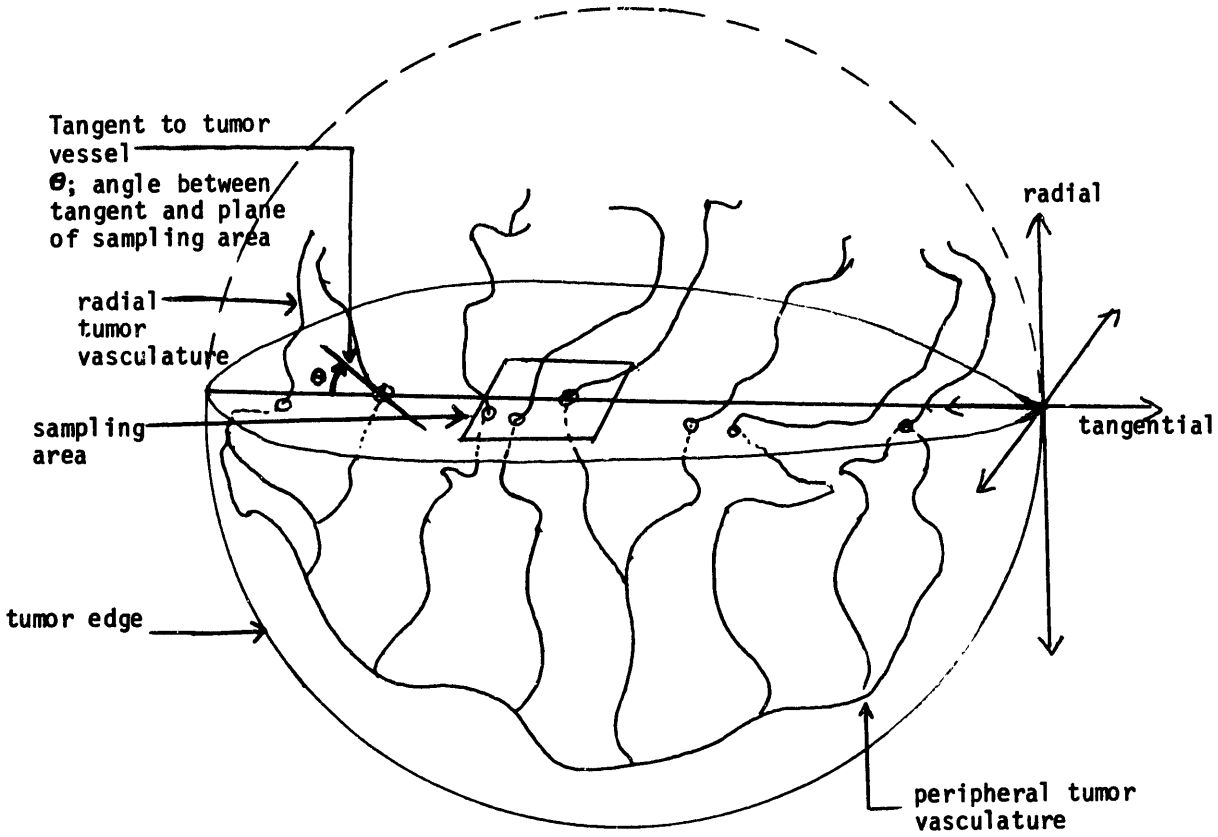

Figure 7: Three dimensional representation of the method of data collection.

(4) The null hypothesis being tested is that there are no radial tumor vessels within the square surface area of 2.5 E+5 um^2 existing inside the renal adenocarcinoma (μ = 0.0 in equation 5). With a standard t-metric test, the acceptance region for the null hypothesis is calculated from equation 5.

(5) Then the experimentally determined mean number of radial tumor vessels(average of 100 data points) is compared with the acceptance region for the null hypothesis.

$$\mu - t_{1-.5\alpha}(d) \cdot s/(n-1)^{.5} < x < \mu + t_{1-.5\alpha}(d) \cdot s/(n-1)^{.5} \qquad (5)$$

where:

x: experimental average number of radial tumor vessels per sample area(100 data points, x_i were averaged)

μ: true mean number of radial tumor vessls per sample area

n: number of trials

s: experimental standard deviation

d = n-1: number of degrees of freedom

(from the definition of t-distribution)

t(d): t-value from t-distribution tables(Duncan,1977)

α: confidence level(e.g. α = 0.05 = 95% confidence interval)

The results of this investigation lead to the rejection of the null hypothesis and acceptance of the alternative hypothesis that inward radial tumor vessels exist with a certainty of at least 95%(α = 0.05). Values for the maximum and minimum true means are calculated using the collected data, x_i, according to equations (6) and (7). The maximum and minimum mean values set the limits on the possible variation in the true mean number of radial tumor vessels for the number of trials performed(n=100) and at the confidence levels stated(95%, 99%). The results of the data analysis are summarized in Table 2.

$$\mu_{min} = x - t_{1-.5\alpha}(d) \cdot s/(n-1)^{.5} \qquad (6)$$

$$\mu_{max} = x + t_{1-.5\alpha}(d) \cdot s/(n-1)^{.5} \qquad (7)$$

Tumor Age (weeks)	Acceptance Interval for Null Hypothesis	x^{**}	μmin	μmax
3	0.0-0.24	3.7	3.46	3.94
4	0.0-0.28	4.4	4.12	4.68
5	0.0-0.40	5.0	4.60	5.40
6	0.0-0.50	6.2	5.70	6.70 95% C.I.
3	0.0-0.32	3.7	3.38	4.02
4	0.0-0.47	4.4	4.03	4.77
5	0.0-0.53	5.0	4.47	5.53
6	0.0-0.66	6.2	5.54	6.86 99% C.I.

** 100 data points were averaged to obtain the numbers in this column

Table 2: Summary of the minimum and maximum true and experimental mean values for all tumor casts examined(the numbers above reflect data obtained from 10 kidney-tumor casts for each tumor age group).

3.2 Thrombin Therapy: A matched pair cohort study

Thrombin, a direct acting coagulant is administered to the center of the tumor necrotic region to examine whether the diffusion of the drug into the tumor vascular network will result in circulatory blockage from vascular thrombosis. Once the vessels are sealed the vascular metastatic process is impeded and tumor perfusion is sharply reduced(i.e. ischemia) leading to increased tumor necrosis.

Table 3 summarizes the tumor diameters at six weeks post tumor implantation(TD 6) and the time to death post tumor implantation(t) as well as the number of open-ended tumor vessels(N) in a fixed 2.5 E=5 um^2 square surface area for both tumor systems and both the thrombin treated and control cohorts.

CONTROL			TREATED	
N	t(days)	Tumor Dia.(cm.) (t = 6 weeks)	N	t(days)
		Renal Adenocarcinoma		
9.5±1.0	72±0.5	4.5±.05	4.8±.47	131±0.5
8.8±.85	73±0.5	4.0±.05	4.1±.39	133±0.5
8.0±.80	75±0.5	3.5±.05	3.4±.35	139±0.5
7.8±.78	76±0.5	3.2±.05	3.3±.30	140±0.5
7.7±.75	78±0.5	2.6±.05	3.1±.28	142±0.5
7.6±.74	78±0.5	2.1±.05	2.9±.27	145±0.5
7.5±.71	80±0.5	1.5±.05	2.8±.25	147±0.5
7.5±.72	81±0.5	1.0±.05	2.7±.26	149±0.5
7.3±.71	80±0.5	.75±.05	2.6±.24	151±0.5
7.2±.70	81±0.5	.50±.05	2.5±.24	154±0.5
		Rhabdomyosarcoma		
8.5±.82	69±0.5	2.5±.05	2.4±.25	89±0.5
7.0±.71	72±0.5	1.6±.05	2.2±.21	91±0.5
6.8±.70	74±0.5	1.2±.05	2.1±.20	94±0.5

Table 3: Summary of the number of open-ended tumor vessels(N), the time to animal expiration post tumor implantation(t), and the tumor diameter pre-thrombin therapy(t=6 weeks) for both tumor systems including the control and treated cohorts.

In the treated cases, therapy is adminstered at six weeks post implantation and polymer casts and histological slides are made at seven weeks post implantation. As mentioned previously, one week is ample time for the thrombin concentration to reach therapeutic levels in the entire tumor region; therfore, the measurement of N after therapy at seven weeks post implantation using histology will reflect the effects of the drug on the status of the open-ended tumor vessels. N is determined by counting the number of polymer(blue) filled vessels per 2.5 E+5 um^2 square surface area on the histology slides.

The square area of 500 um x 500 um is selected to ensure that within any area of evaluation there will be at least one data point. The determination of the dimensions of the sample area was previously explained. Figure 8 is a histological cross section of renal adenocarcinoma taken after both thrombin therapy and polymer injection.

Figure 8: Medial cross section of renal adenocarcinoma after therapy(t= 6 weeks) and casting(t= 7 weeks). Note the appearence of both clotted tumor blood vessels(red) and polymer filled(blue) blood vessels within the 2.5 E+5 um^2 sample area.

Figure 8: Medial cross section of renal adenocarcinoma after therapy(t= 6 weeks) and casting(t= 7 weeks). Note the appearence of both clotted tumor blood vessels(red) and polymer filled(blue) blood vessels within the 2.5 E+5 um^2 sample area.

Note the presence of both polymer filled(blue) and thrombosed(red) blood vessels. Only those vessels that remain open after therapy will provide access for polymer infusion after its administration to the center of the tumor necrotic region. Also, illustrated in figure 2b(also figure 7) is the square sampling area used to collect data(N) on the number of open-ended tumor vessels.

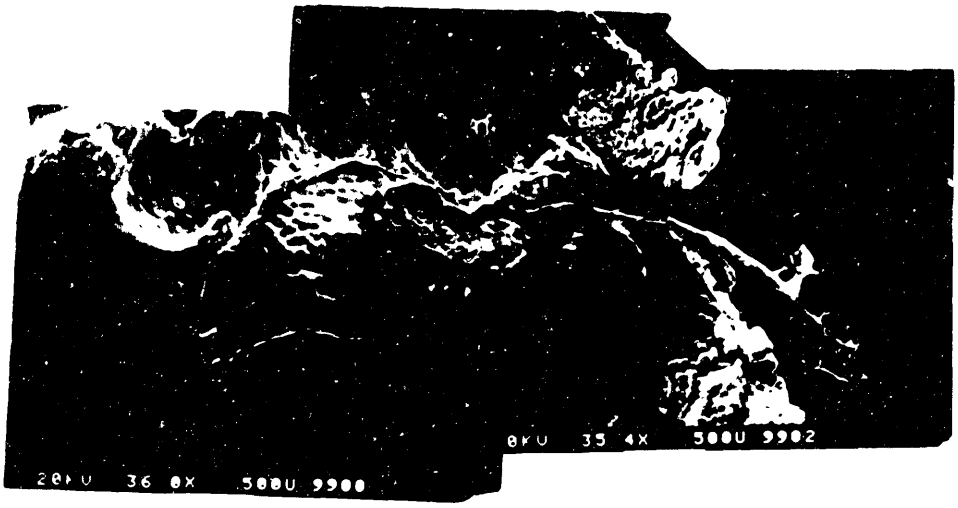

Figure 9: A scanning electron micrograph of a polymer casted 3.5 cm diameter renal adenocarcinoma taken after treatment. Note, the finger like projections(open-ended blood vessels) extending from the central polymer mass(necrotic region).

Note the presence of both polymer filled(blue) and thrombosed(red) blood vessels. Only those vessels that remain open after therapy will provide access for polymer infusion after its administration to the center of the tumor necrotic region. Also, illustrated in figure 2b(also figure 7) is the square sampling area used to collect data(N) on the number of open-ended tumor vessels.

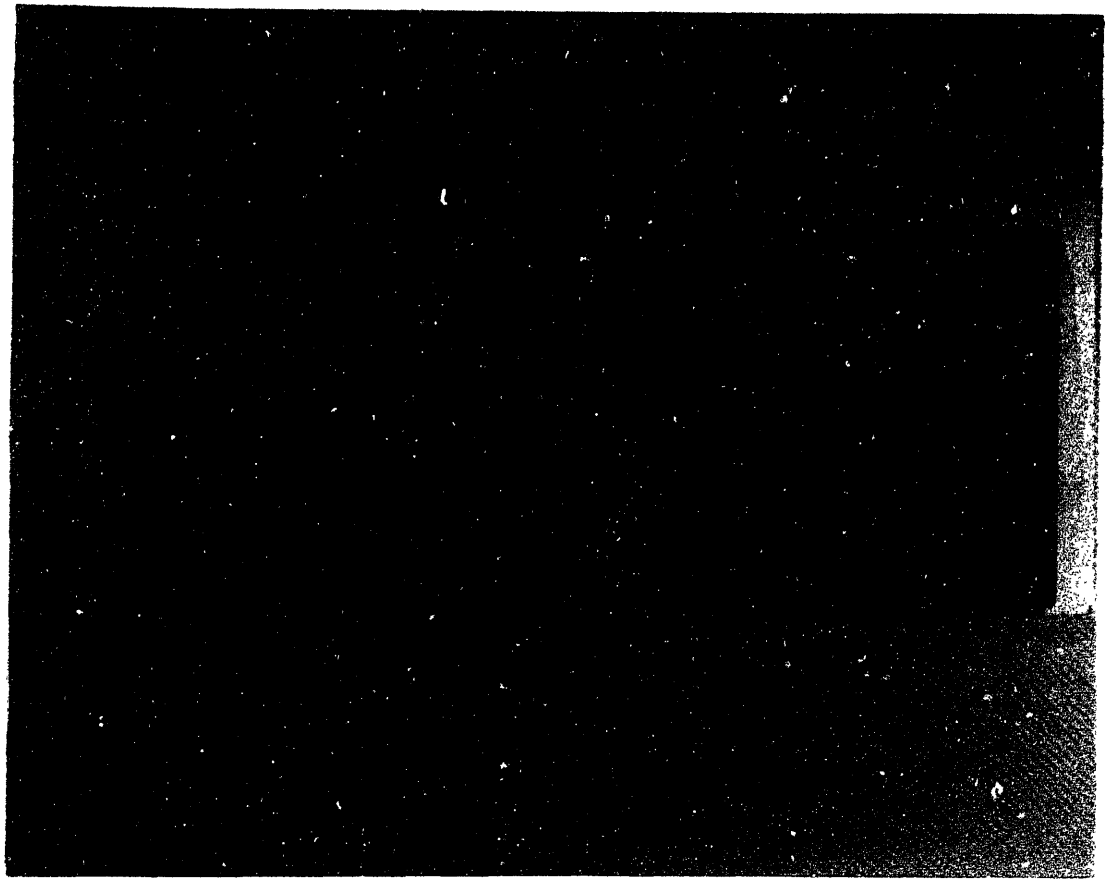

Figure 9: A scanning electron micrograph of a polymer casted 3.5 cm diameter renal adenocarcinoma taken after treatment. Note, the finger like projections(open-ended blood vessels) extending from the central polymer mass(necrotic region).

Figure 9 is one representative electron micrograph showing a polymer casted specimen. Note the central region of polymer that fills the necrotic region of the tumor, and the finger like protrusions extending from the central polymer mass. These protrusions are pathways which provided an outlet through which the polymer could flow. A careful investigation of the surface morphology of the casts(i.e examination for endothelial cells) shows that these cylindrical structures are blood vessels. Therefore, in order for the polymer to enter these vessels they would have to be open-ended.

The results in table 3 for N and t are evaluated using a students t-metric (for a matched pair study) to test the following null hypotheses:

$^{1}H_{o}$: There is no difference in the time,'t' to animal death(lung metastasis) between the control and treated cohorts.

$^{2}H_{o}$: There is no difference in the number of open-ended tumor vessels, 'N' in the control and treated cohorts.

The statistical test is performed on each pair of control-treated data pairs that were matched for tumor diameter at t=6 weeks(pre-treatment). The matching ensured that the tumor geometry at the cellular and vascular levels were comparable before therapy. The student t-metric for a matched pair study is used in the evaluation and is given by:

$$t = x/(s/(n)^{.5}) \quad (8)$$

where:

x: mean difference in the variable(N,t) before(control) and after treatment.

s: standard deviation in the difference results

n: number of trials

The results of the test show that with at least 99% certainity there is a significant difference in the treated and control groups values for N and t. Specifically, the treated group had a larger time to animal death(lung metastasis) and a lower number of open-ended tumor vessels. The 99% confidence intervals for the difference in N and t between the control and treated cohorts are as follows:

Adenocarcinoma:

t: [61.16, 70.24] with mean = 65.7 days

N: [4.59, 4.75] with mean = 4.61

Rhabdomyosarcoma:

t: [16.37, 22.97] with mean = 19.67 days

N: [0.78, 9.62] with mean = 5.2

4. DISCUSSION OF RESULTS

In this section the morphological details of tumor vasculature are examined. A vascular metastatic pathway is established and the efficacy of thrombin as a new cancer chemotherapeutic agent is investigated.

4.1 Tumor Versus Renal Vascular Morphology

It is instructive to examine some relevant features of normal kidney vasculature and compare these features with those of tumor vasculature. Figure 10 shows normal kidney vasculature.

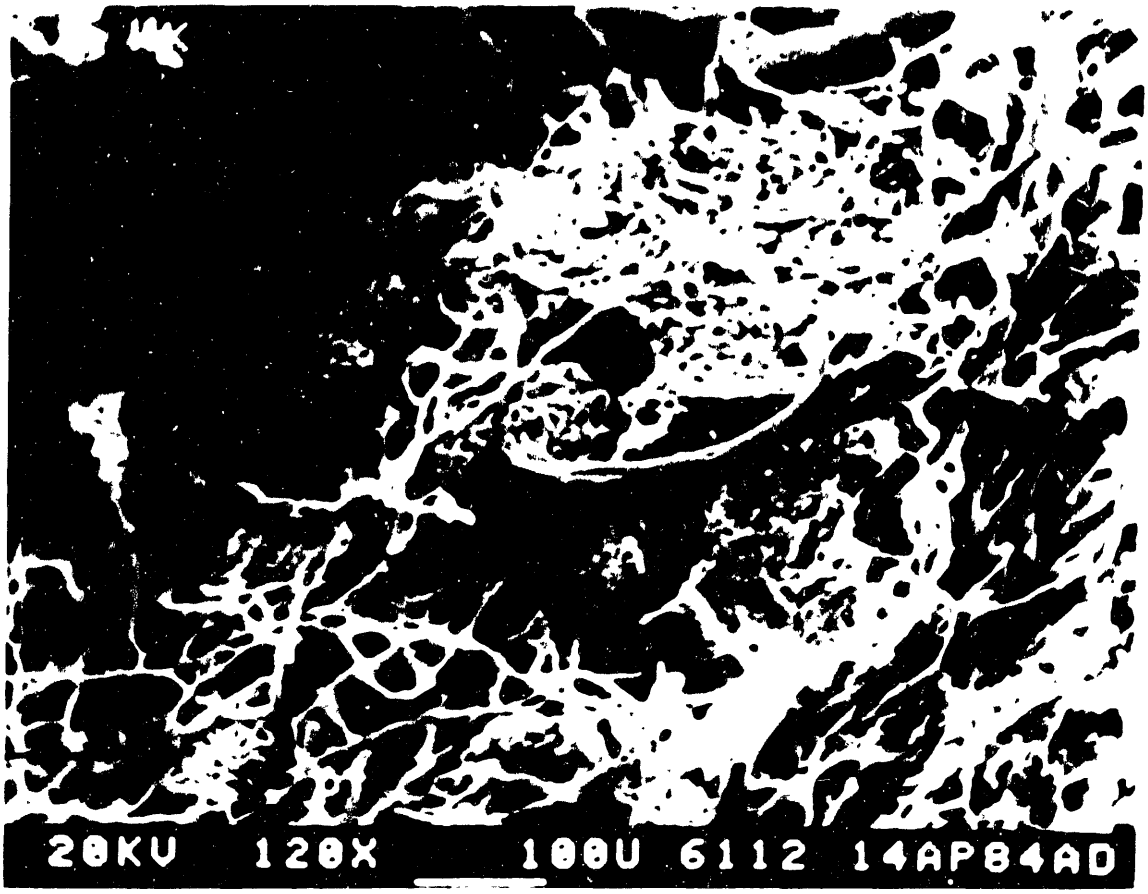

Figure 10: Micrograph of normal kidney vasculature.

Note that this vasculature is organized in parallel sets of capillaries that gather at masses called glomeruli. The glomerulus is a tuft of capillary loops projecting into the expanded end (Bowman's capsule) of each of the uriniferous tubules. Another feature of the

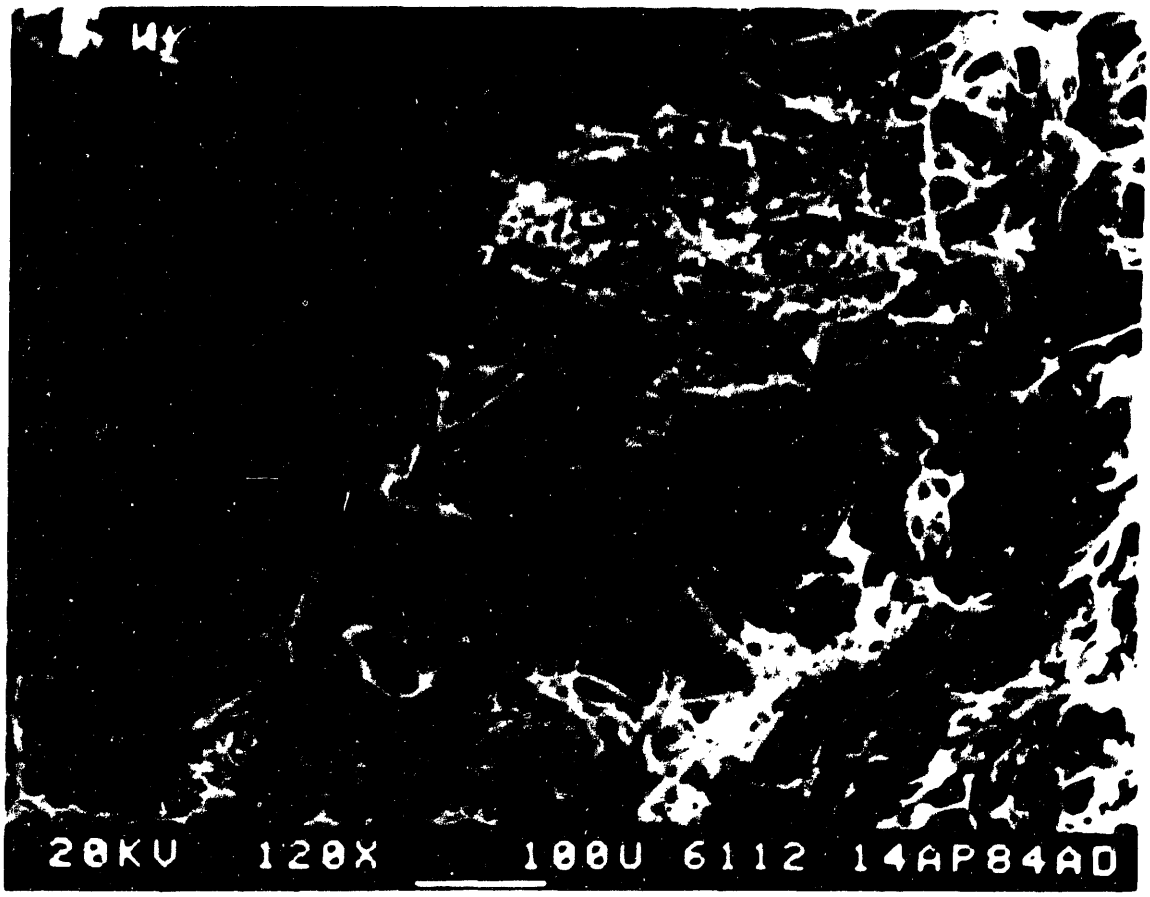

Figure 10: Micrograph of normal kidney vasculature.

Note that this vasculature is organized in parallel sets of capillaries that gather at masses called glomeruli. The glomerulus is a tuft of capillary loops projecting into the expanded end (Bowman's capsule) of each of the uriniferous tubules. Another feature of the

Figure [illegible]: Example of [illegible]. The interface between the [illegible]. Note [illegible]

comparison is that the diameter of the normal kidney vasculature is similiar to that of tumor microvasculature, being not less than 10 um. In contrast, the tumor microvasculature in Figures 11, 12a, 12b, and 13 show noteworthy features that differ from those of the normal kidney vessels. These dissimilarities include the following:

(1) A major vessel can have multiple branches(Figure 11).

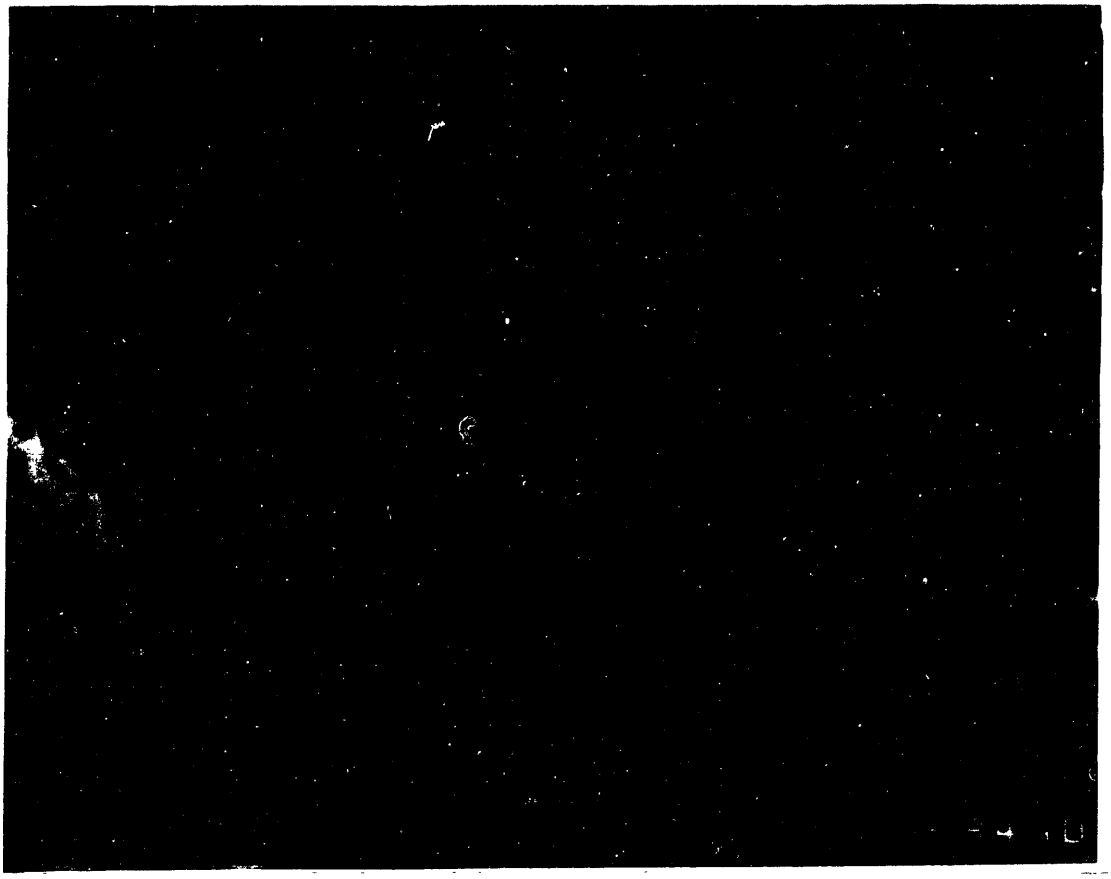

Figure 11: Example of sprouting found in tumor microvasculature. The interface between the kidney and tumor is depicted. Notice the inward pointing tumor vasculature and sprouting vascular buds.

(2) In conjunction with statement (1), there are mitotic endothelial cells located on small buds sprouting off the main vessel. Mitotic endothelial cell imprints are distinct from resting endothelial cell imprints in that they show a smooth but indented surface due to a nuclear bulge(figure 12a, 12b). The presence of these mitotic cells suggests that a growing vessel stems from the location of the mitotic capillary endothelial cells. As mentioned in the introduction, this growth may be stimulated by and directed towards tumor cell secreted TAF(Folkman, 1975).

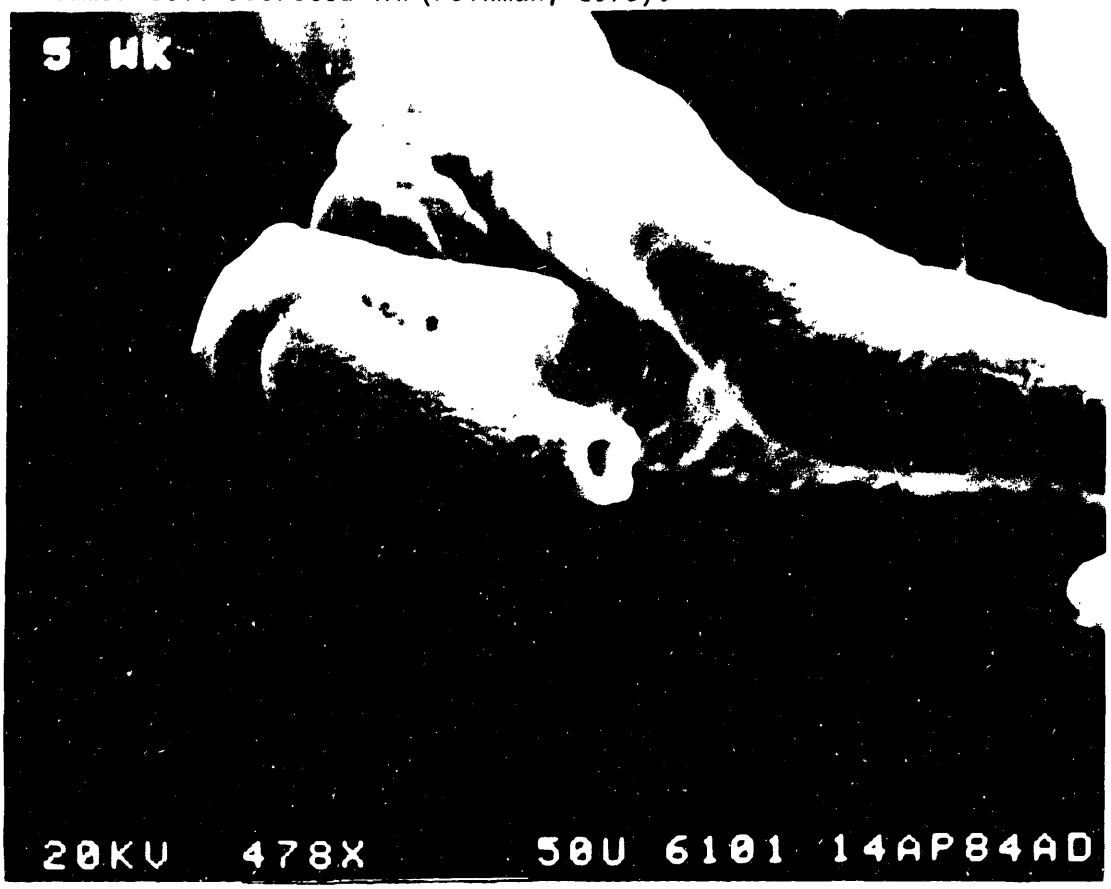

Figure 12a: Micrograph of endothelial cell nuclei located on small buds sprouting off the main vessel.

(2) In conjunction with statement (1), there are mitotic endothelial cells located on small buds sprouting off the main vessel. Mitotic endothelial cell imprints are distinct from resting endothelial cell imprints in that they show a smooth but indented surface due to a nuclear bulge(figure 12a, 12b). The presence of these mitotic cells suggests that a growing vessel stems from the location of the mitotic capillary endothelial cells. As mentioned in the introduction, this growth may be stimulated by and directed towards tumor cell secreted TAF(Folkman, 1975).

Figure 12a: Micrograph of endothelial cell nuclei located on small buds sprouting off the main vessel.

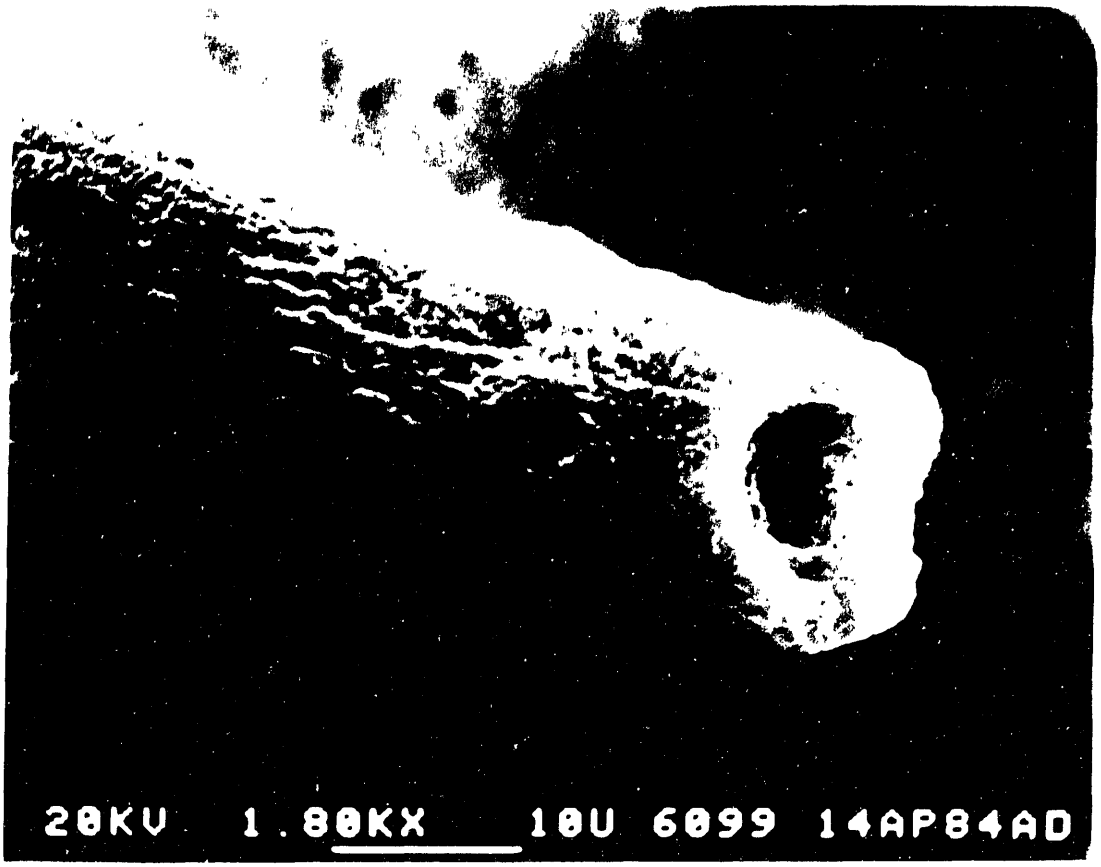

Figure 3.1: Higher magnification view of endothelial cell nucleus located on wall branch arising off the main vessel.

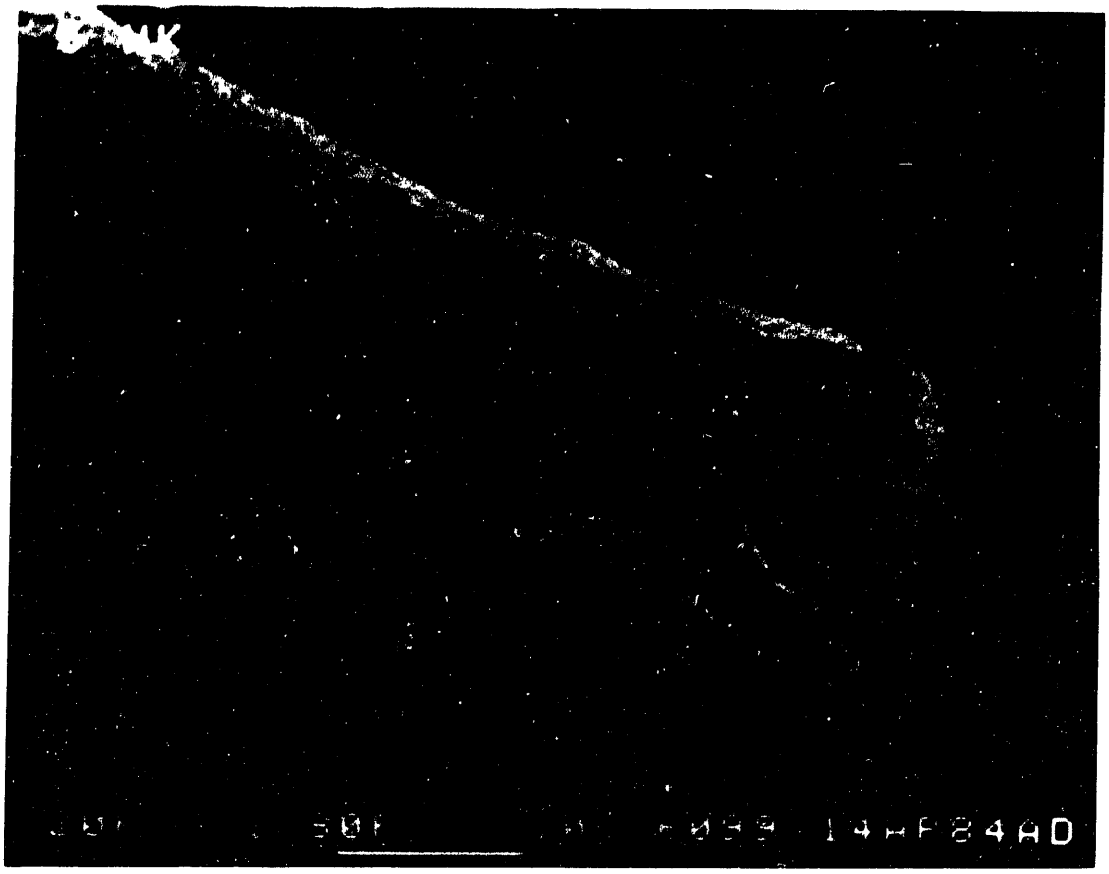

Figure 12b: Higher magnification view of endothelial cell nuclei located on small buds sprouting off the main vessel.

(3) Mitotic endothelial cells are also located on the periphery of some tumor vessels, indicating direct growth(Figure 13). The indented region on the outer perimeter of the tumor blood vessel is exemplary of a mitotic endothelial cell.

From Figure 11 and other work(Shah, 1983; Babayan, 1984; Nelson, 1984) it is apparent that the tumor vasculature near the kidney tumor interface is composed of kidney vasculature which is initially normal and then becomes altered due to the presence of the growing tumor. Figure 14 shows the kidney-tumor interface from a 6 week tumor cast. In this figure one observes the presence of modified kidney vasculature(diameter approximately 10-40 um) and the proliferation of new tumor capillaries(diameter approximately 10 um) both at the kidney-tumor interface.

Figure 13: Radial growth is suggested by the endothelial cell(indentation in cast) located on the periphery of the tumor capillary.

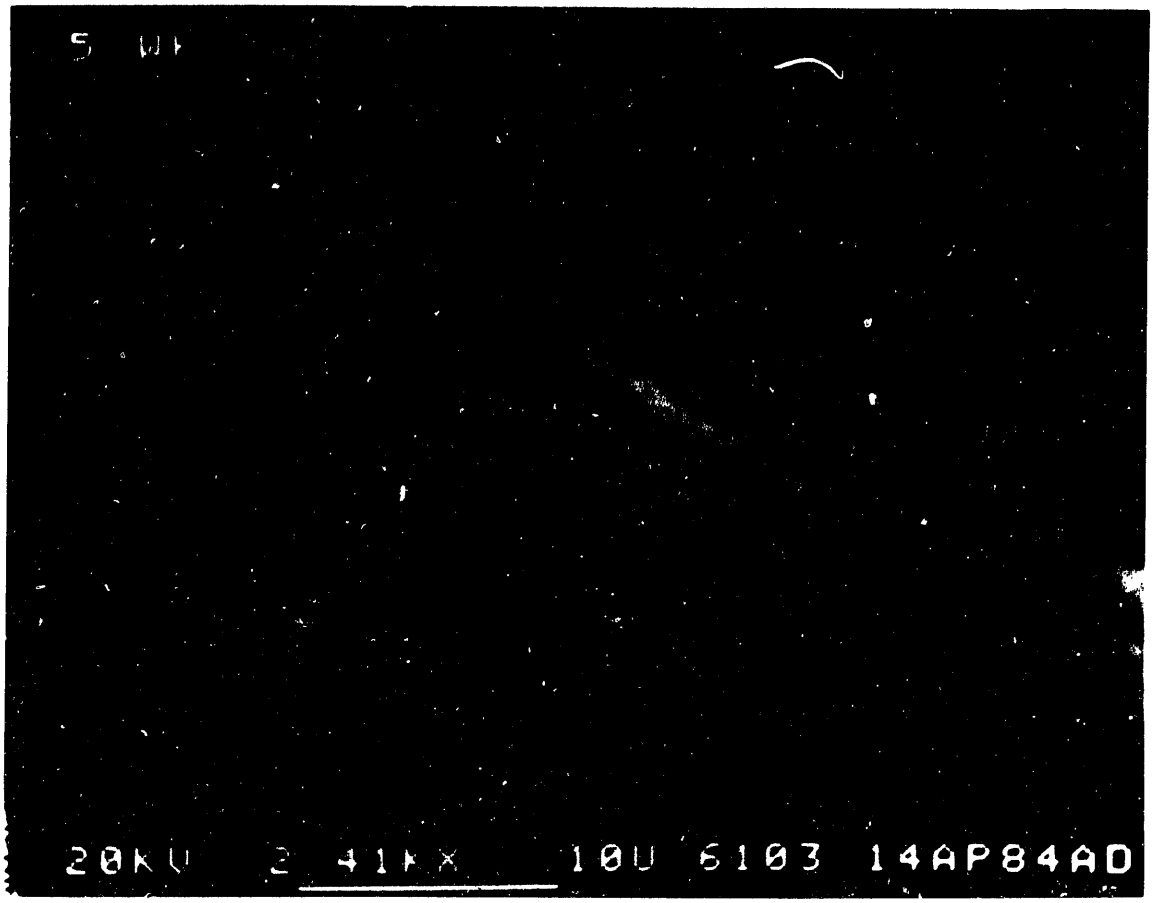

Figure 13: Radial growth is suggested by the endothelial cell(indentation in cast) located on the periphery of the tumor capillary.

Figure 14: Micrograph of modified kidney vasculature(diameter approx. 10-40 um) and new tumor capillaries(diameter approx. 10 um) at the kidney-tumor interface.

Figure 14: Micrograph of modified kidney vasculature(diameter approx. 10-40 um) and new tumor capillaries(diameter approx. 10 um) at the kidney-tumor interface.

4.2 A Vascular Metastatic Pathway

Apparently two classes of radial tumor vessels exist. The first class depicted in figures 11, 12a, 12b, and 13 seems to be comprised of vessels growing radially inward and which are closed-ended. The second class depicted in figures 15 and 16 appears to be comprised of vessels that are dying, open-ended and are proximally located to the tumor necrotic region.

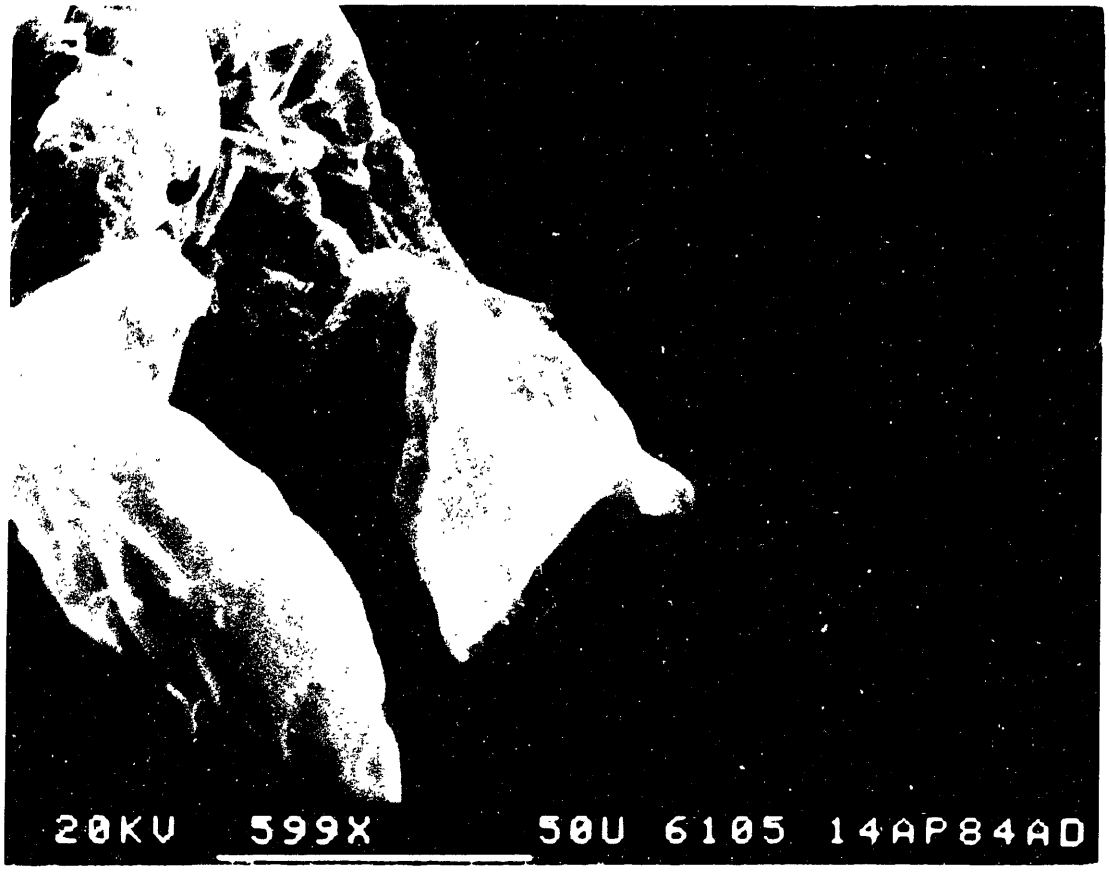

Figure 15: An open-ended dying tumor capillary(diameter approx. 10um) located adjacent to the tumor necrotic zone(dark portion of micrograph in lower right).

4.2 A Vascular Metastatic Pathway

Apparently two classes of radial tumor vessels exist. The first class depicted in figures 11, 12a, 12b, and 13 seems to be comprised of vessels growing radially inward and which are closed-ended. The second class depicted in figures 15 and 16 appears to be comprised of vessels that are dying, open-ended and are proximally located to the tumor necrotic region.

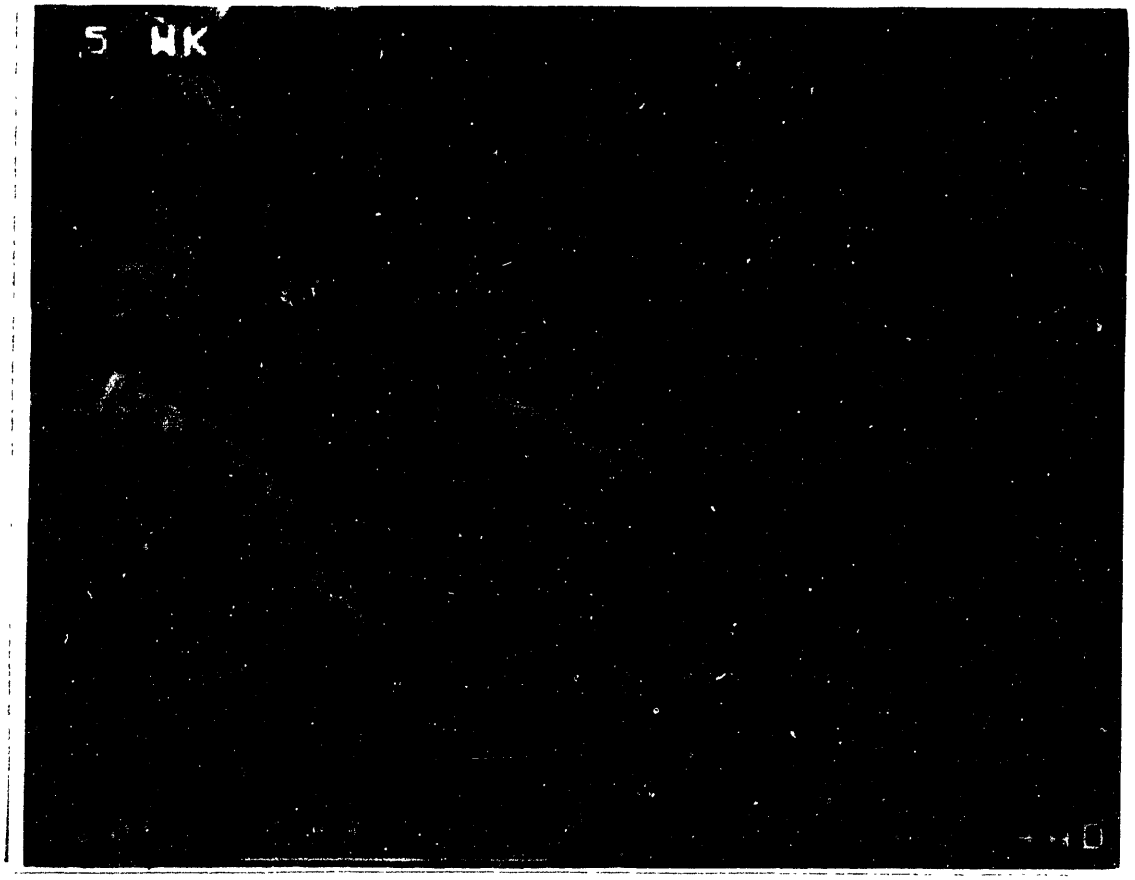

Figure 15: An open-ended dying tumor capillary(diameter approx. 10um) located adjacent to the tumor necrotic zone(dark portion of micrograph in lower right).

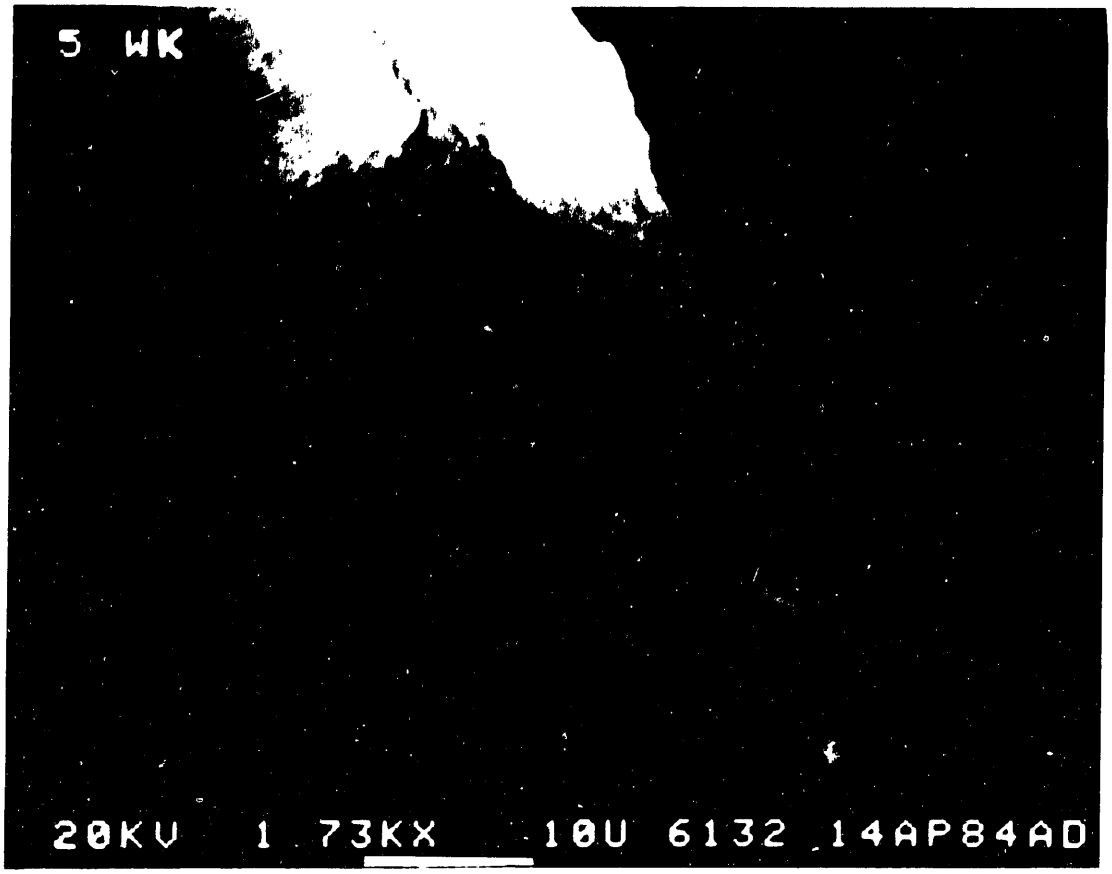

Figure 16: An illustration of a branched tumor vessel located partially within the necrotic region which is in the process of collapsing and becoming open-ended.

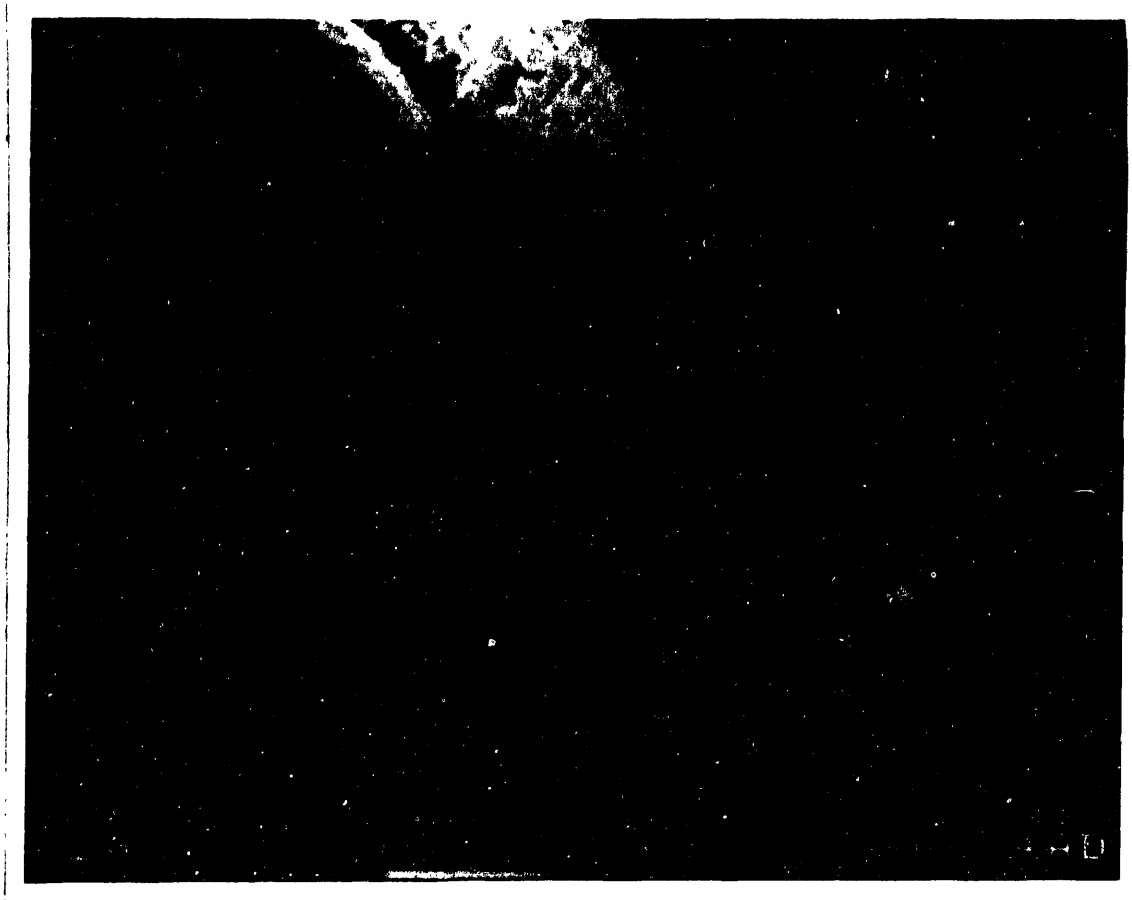

Figure 16: An illustration of a branched tumor vessel located partially within the necrotic region which is in the process of collapsing and becoming open-ended.

A plausible explanation for the existence of two types of tumor vessels is illustrated in figure 2b. Note that the closed-ended tumor vessels are growing radially inward and are located distally from the outer surface of the tumor necrotic region. This class of vessels stems from larger diameter peripheral tumor vessels located in the oxygenated circumferential region of the tumor. The open-ended tumor vessels are located proximally to the tumor necrotic region. It is proposed that as the necrotic region enlarges, those engulfed vessels or pieces of vessels within the growing necrotic volume will decompose, resulting in apparently open-ended(i.e. terminated or dead end) tumor vasculature in the 'non-necrotic' region of the tumor mass. The open-ended tumor vessel system is interconnected to the larger diameter tumor vessels located in the well oxygenated periphery of the tumor. These larger vessels are connected to the renal vasculature which leads to the inferior vena cava via the renal vein. In summary, the open-ended vessels can serve as a pathway leading to the main circulatory system from the primary tumor mass as previously stated in the introduction as the hypothesis.

The cancer cells that have access to the open-ended vessel network are likely to be in the hypoxic region of the tumor,(i.e. the region surrounding the anoxic tumor necrotic region) and as a result are probably in a resting phase. The resting phase exists because the region directly adjacent to the tumor necrotic region is of low oxygen tension,

hypoglycemic, and lacking in other needed cell nutrients due to inadequate perfusion to this tumor region(Weiss, 1978). If these cells are exposed to adequate oxygen tension and other needed nutrients they can eventually begin to proliferate(Kallman, 1972). Therefore, if one or more of these resting cells entered the open tumor vessel pathway, it can travel to adequately perfused regions of the tumor, renal vasculature, or even the main circulatory system. In these regions of sufficient nutrient supply the resting cells could begin to proliferate and potentially create a microtumor which could travel through the vascular system and subsequently be trapped in the vascular endothelium at the secondary metastatic site.

4.3 Evidence for the Proposed Metastatic Pathway

The behavior of both N, the number of open-ended tumor vessels and t, the time to animal expiration post tumor implantation observed after thrombin therapy suggests that tumor vasculature is involved in the metastatic process. Table 4 lists the percentage change in N and t after therapy for each matched data pair. The percentage change is given by equation 9.

$$\% \text{ change} = [(X'-Xo)/Xo] \times 100 \qquad (9)$$

where:

Xo: Value of variable before treatment(Control cohort)

X': Value of variable after treatment (Treated cohort)

Tumor Diameter(cm) (t = 6 weeks)	N'-No	t'-to (days)	(N'-No)/(No) x 100	(t'-to)/(to) x 100
Renal Adenocarcinoma				
4.5	-4.7	59.0	-49.5%	81.9%
4.0	-4.7	60.0	-53.4%	82.2%
3.5	-4.6	64.0	-57.5%	85.3%
3.2	-4.5	64.0	-57.6%	84.2%
2.6	-4.6	64.0	-59.7%	82.1%
2.1	-4.7	67.0	-61.8%	85.9%
1.5	-4.7	67.0	-62.7%	83.8%
1.0	-4.8	68.0	-64.0%	84.0%
0.75	-4.7	71.0	-64.4%	88.8%
0.50	-4.7	73.0	-65.3%	90.1%
Rhabdomyosarcoma				
2.5	-6.1	20.0	-71.8%	29.0%
1.6	-4.8	19.0	-68.6%	26.4%
1.2	-4.7	20.0	-69.1%	27.0%

Table 4: Summary of the Difference and the Difference percent for the time to animal expiration and the number of open-ended tumor vessels between control and treated pairs matched for tumor diameter at t = 6 weeks post implantation.

Thus the significant decrease in N and the pronounced increase in t after thrombin therapy suggests that the tumor vessel network is involved in the vascular metastatic pathway. Furthermore, the data suggests that this pathway can be blocked via vascular thrombosis using a direct acting coagulant such as thrombin.

To establish a functional relationship between the morphology of the tumor vessel network and the time to vascular metastasis a formula is derived relating the number of open-ended tumor vessels to the time to metastasis using Poisson statistics and first order kinetics. The formula is then tested with the data obtained in this study(plotted in Figures 17 a,b;18 a,b) with a non linear regression analysis(Bevington, 1969).

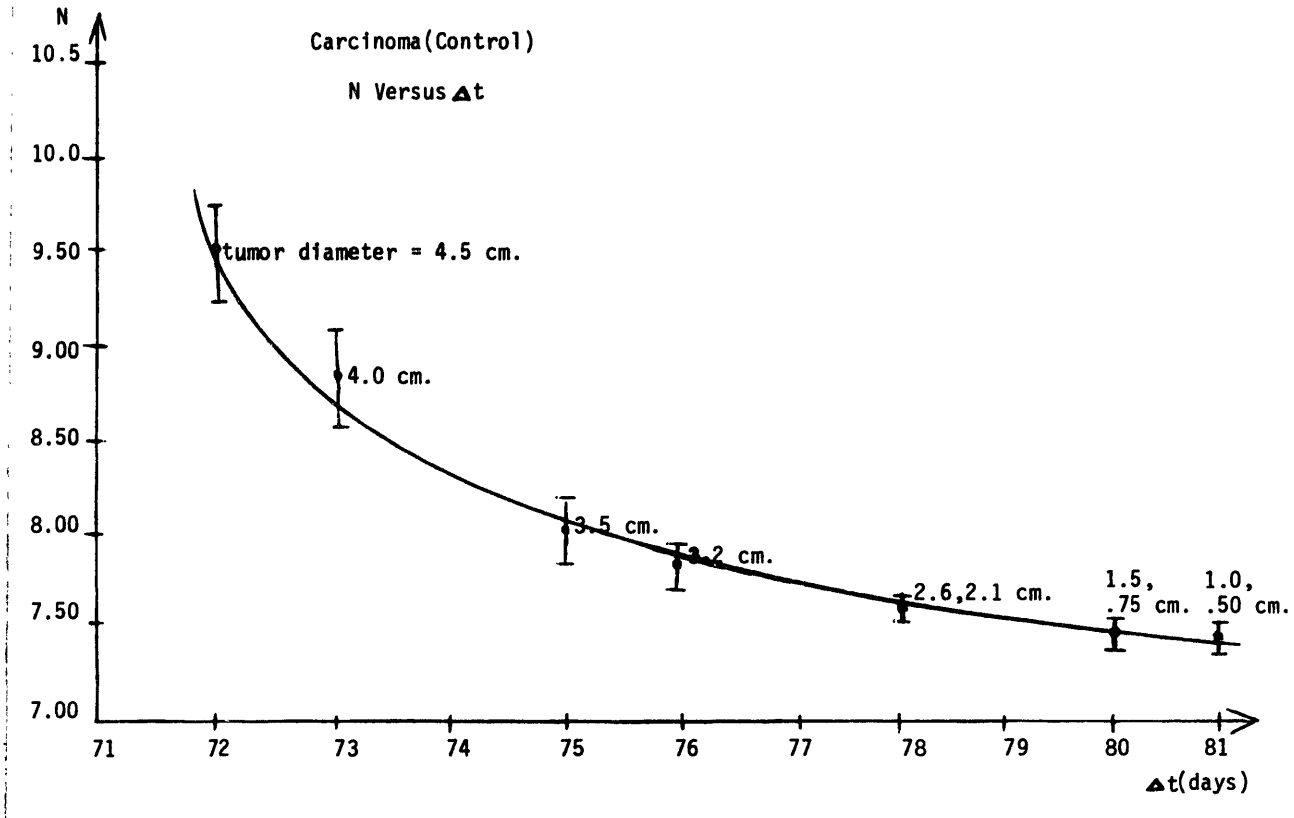

Figure 17a: Graph of N versus t for Renal Adenocarcinoma(Control).

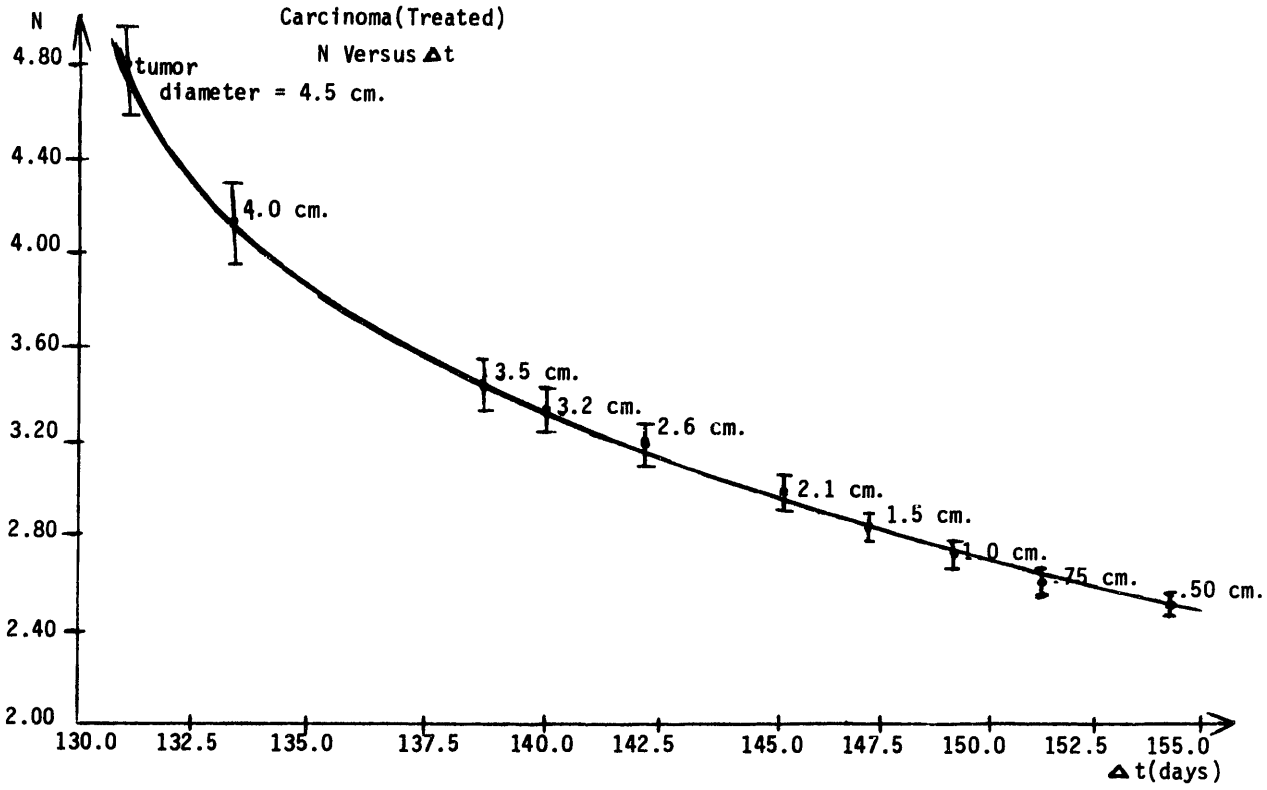

Figure 17b: Graph of N versus t for Renal Adenocarcinoma(Treated).

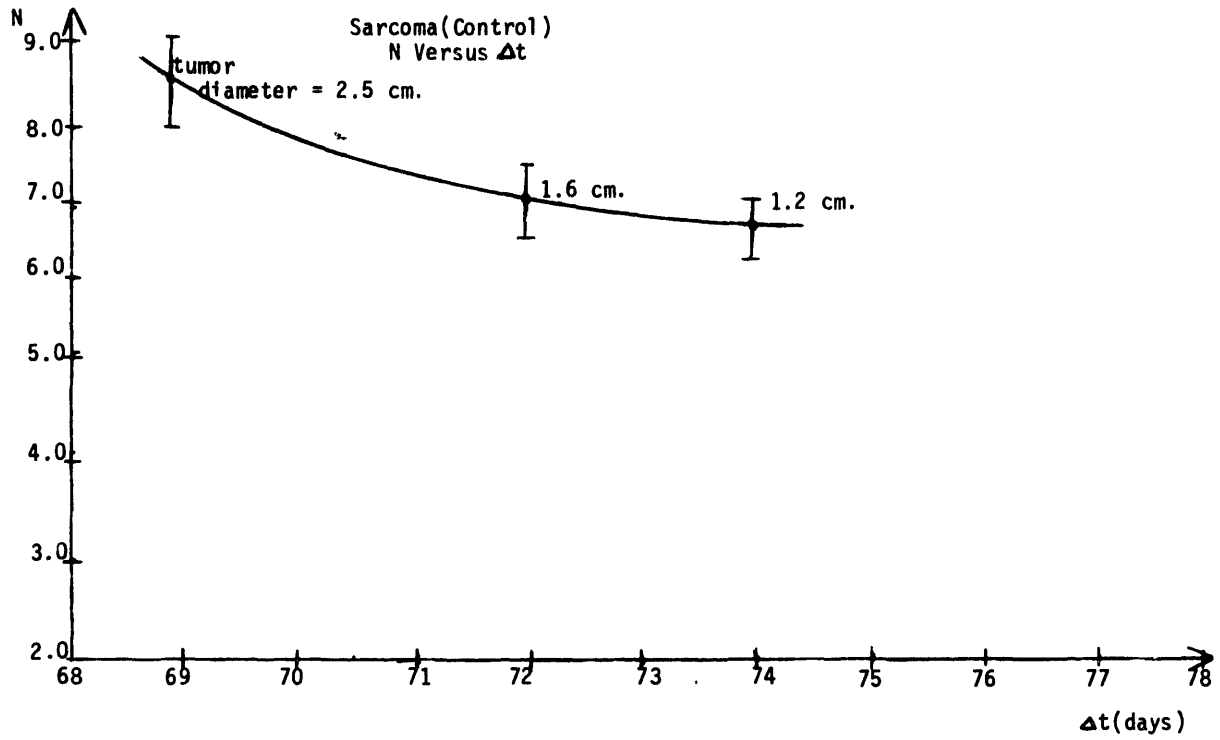

Figure 18a: Graph of N versus t for Rhabdomyosarcoma(Control).

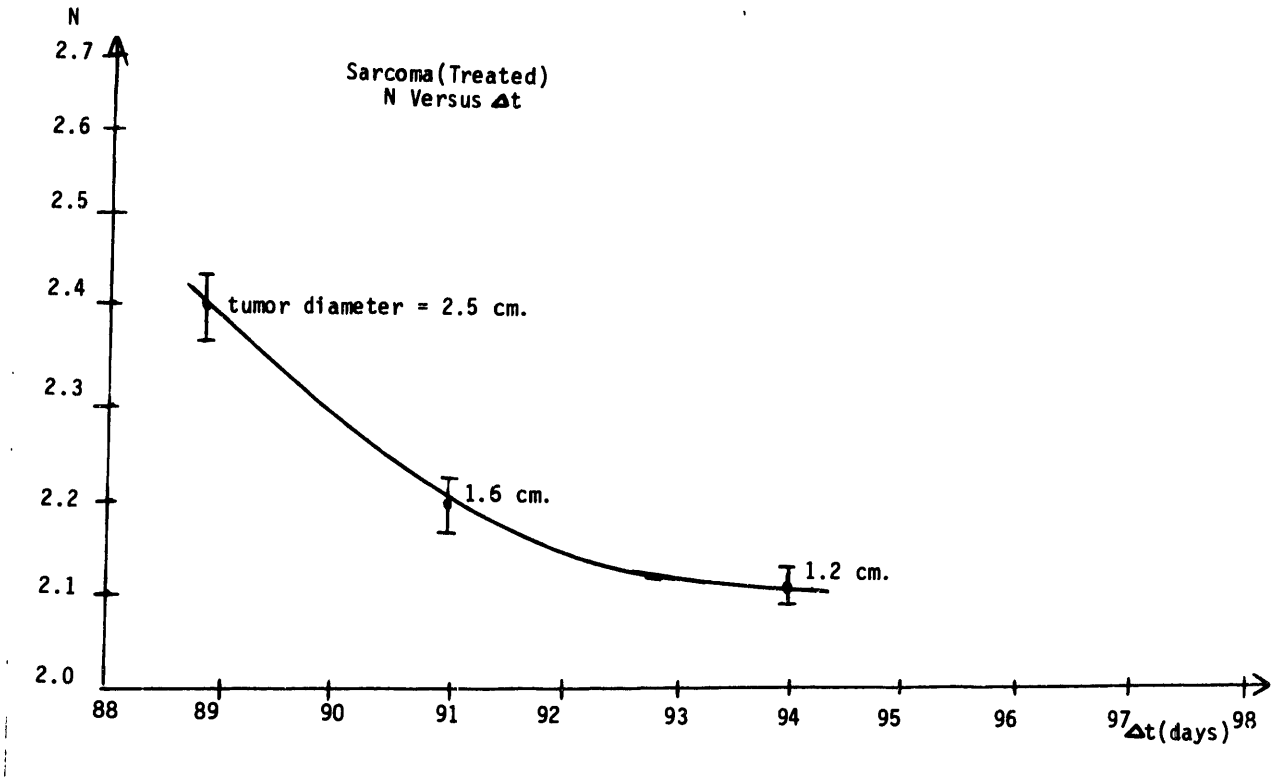

Figure 18b: Graph of N versus t for Rhabdomyosarcoma(Treated)

Because the number of open-ended vessels(N) per unit radius(r) decreases linearly as the local thrombin concentration, C(r,t) increases.

$$dN(r,t)/dr = -kC(r,t) \qquad (10)$$

where:

k: rate constant(in cm^2)

C(r,t): concentration profile given in equation 1.

Now integrate both sides of equation (10) with respect to r over all possible tumor diameters leaving only the t dependence of N given by:

$$N(t) = \int_{r=0}^{r=\infty} dN(r,t)/dr \cdot dr = -k\int_{r=0}^{r=\infty} C(r,t)dr \qquad (11)$$

Integrating leads to:

$$N(t) = 15kU/16\pi Dt \qquad (12)$$

where:

D: thrombin diffusion coefficient in blood(cm^2/sec)

U: the number of units of thrombin administered

t: time post thrombin therapy

One can relate the uncertainity in the measurement of N to the uncertainity in the measurement of t as follows:

$$(\sigma_N)^2 = (dN(r,t)/dt)^2 \cdot (\sigma_t)^2 \qquad (13)$$

where:

σ_N : standard deviation in N

σ_t : standard deviation in t

Differentiate equation (12) and substitute into equation (13) to obtain:

$$(\sigma_N)^2 = (\sigma_t)^2 \cdot [5/256(kU/\pi D)^2]t^{-2} \qquad (14)$$

Because the sampling size for N(100 samples per data point) is large and any given value of N is small, Poisson sampling statistics is valid for the measurement of N and therefore:

$$\sigma_N = (N)^{.5} \qquad (15)$$

Finally, equating equations (14) and (15) gives the predicted inverse square relationship between N and t as follows:

$$N = (\sigma_t)^2 \cdot [5/256(kU/\pi D)^2]t^{-2}$$

Since, $\Delta t = t-2$ weeks

where Δt: time to metastasis

We have the final result that:

$$N \propto 1/(\Delta t)^2 \qquad (16)$$

The relationship in equation (16) is tested using regression analysis and the correlation coefficients for both tumor systems and groups(treated, control) are listed in Table 5.

Tumor Type	Mode	r(correlation coefficient)
Adenocarcinoma	Control	0.950
Rhabdomyosarcoma	Control	0.970
Adenocarcinoma	Treated	0.999
Rhabdomyosarcoma	Treated	0.970

Table 5: Listing of the correlation coefficients obtained from non-linear regression analysis of N proportional to $(t)^{-2}$ for both tumor systems and control and treated cohorts.

The results indicate that a significant(>95% confidence) correlation of the type expressed in equation (16) exists. Therefore, the theoretical relationship between N and t is supported by our experimental results. Furthermore, an inverse square relationship between N and t indicates that by DECREASING N(e.g. via vascular thrombosis) the VASCULAR METASTATIC PATHWAY is INHIBITED resulting in a substantial TIME DELAY in the occurrence of METASTASIS.

4.4 Cellular Detachment and Vascular Metastasis

An important question to be addressed concerns cellular detachment within the tumor. The resting stage cells located in the tumor hypoxic region and directly exposed to the open-ended vasculature must somehow detach from their location before entering the open-ended vessels. The mechanism for this detachment is believed to be due to the action of active lysosmal enzymes present in the tumor necrotic region(Weiss, 1978; Turner, 1980). These enzymes can promote necrotic infiltration by lysing neighboring cells and thereby increasing the spread of the cellular lysosomal contents, and they can degrade the connective tissue matrix that secures the hypoxic cells, thus permitting cells to move freely and enter the nearby open-ended tumor vessels. Two forces are present which can act to allow movement of the detached cells into the open-ended vessels, namely, reaction force and Bernoulli force.

4.4a A Reaction Force

The first force is a reaction force which originates at the center of mass of the tumor and is directed outward toward the tumor periphery (Figure 19).

This force develops in response to the force applied by the elastic membrane (i.e. renal capsule) which is acting normal to the kidney surface and inward. The outward tumor growth will be limited by the elasticity and maximum growth rate of the renal capsule and, as a result, eventual invasion of the tumor mass into the kidney cortex will occur.

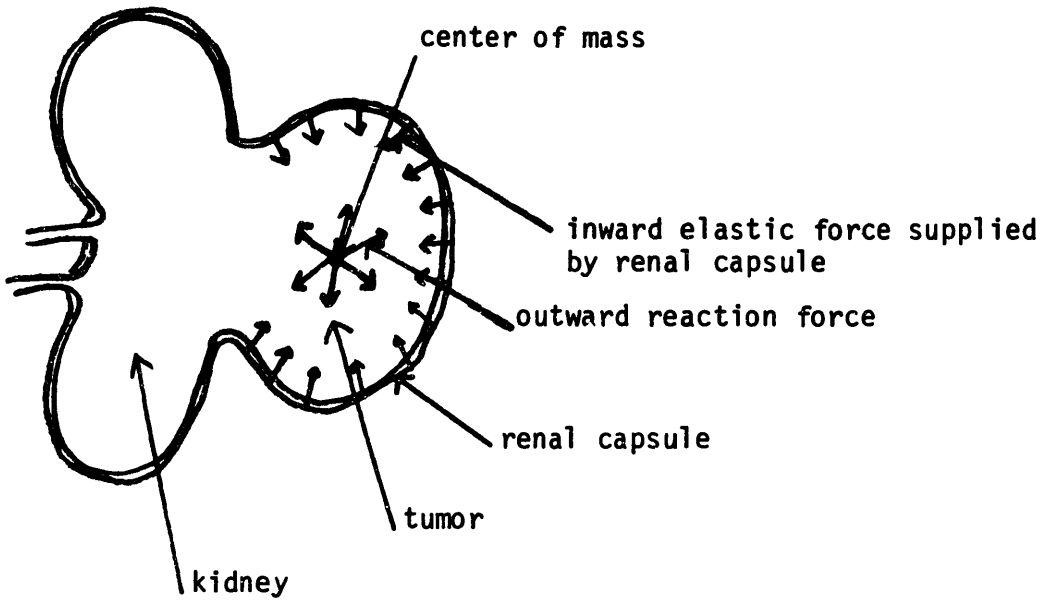

Figure 19: Illustration of the generation of the outward reaction force acting in opposition to the applied inward elastic membrane force.

4.4b Bernoulli Pressure Gradient

The Bernoulli pressure gradientcan generate a force as follows:

For a laminar stream of blood flow through a peripheral tumor vessel one can define a fluid pressure, P_1, velocity V_1, and height h_1 on a streamline such that:

$$P_1 + .5\rho_1(V_1)^2 + mgh_1 = \text{Constant} \qquad (17)$$

Similarly for an open-ended tumor vessel branching from one such peripheral vessel(Figure 20) one can define P_2, V_2, and h_2 on a given streamline as in equation 17 so that:

$$P_2 + .5\rho_2(V_2)^2 + mgh_2 = \text{Constant} \qquad (18)$$

Note that:

$$h_1=h_2,\ V_1=0 \text{ cm/sec},\ \rho_1=\rho_2=\rho_{blood}=1.003 \text{ gm/cm}^3,\ V_2=11 \text{ cm/sec}$$

After equating equations 17 and 18 and using the above values for the parameters one finds that:

$$\Delta P = P_2-P_1 = .5\rho_2(V_2)^2 \simeq 100 \text{ torr(radially outward)}. \qquad (19)$$

$$\Delta P = P_2 - P_1 = .5\rho_2(V_2)^2 \simeq 100 \text{ torr.} \quad (19)$$

Therefore, a driving pressure of 100 torr as well as a reaction force due to the tumors encapsulation in an elastic membrane both act on the loosely attached tumor hypoxic cells to direct their movement towards and into the open-ended tumor vessel network. Once in the tumor vasculature, the cancer cells can travel via the blood stream to the main circulatory system thus creating the possibility of metastasis.

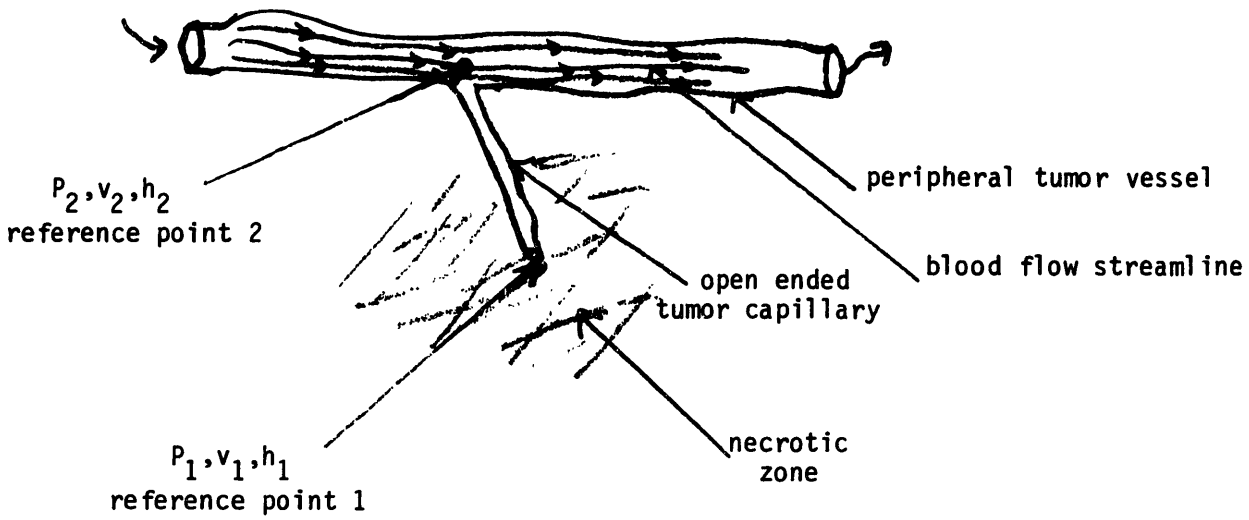

Figure 20: Illustration of the Bernoulli pressure gradient and resulting outward force generated from the blood flow velocity differences in class 1 and class 2 tumor blood vessels.

4.5 Thrombin Therapy's Efficacy and Clinical Usefullness

In addition to decreased tumor perfusion induced by vascular thrombosis increased ischemia results in tumor cell anoxia and necrosis. The necrosis then spreads through the action of lysosomal enzymes in the tumor necrotic zone(Weiss, Turner 1978,1980) which promotes necrotic infiltration by lysing neighboring cells and thereby releasing additional lysosomal contents throughout the tumor mass(Autolysis, Figure 21).

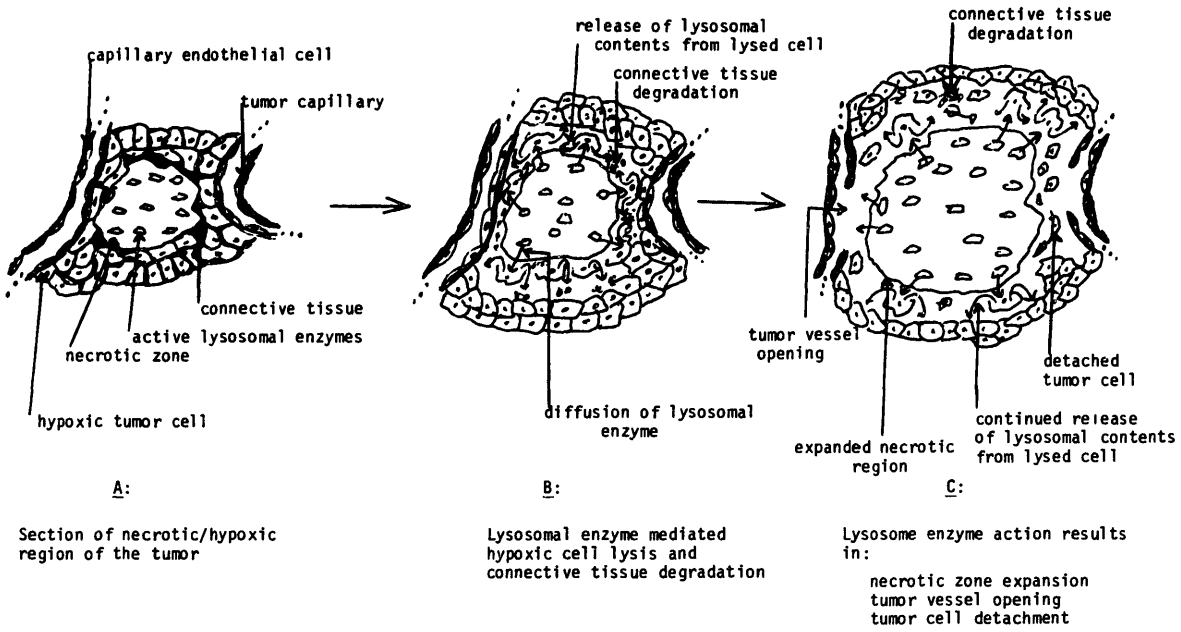

Figure 21: Illustration of lysosomal enzyme action on tumor necrosis and connective tissue degradation.

Thrombin therapy enhances peripheral cell death caused by decreased perfusion and this, coupled with necrotic infiltration arising from the diffusion of active lysosmal enzymes throughout the tumor mass, results in the efficient elimination of the primary tumor from both the inside out and the outside in. Specifically, upon examination one week after thrombin therapy it is found that the renal adenocarcinoma tumor volume has decreased by (53.9 $\pm$ 0.7)% and the rhabdomyosarcoma tumor volume has decreased by (43.9$\pm$ 0.5)% on average indicating cell anoxia has lead to substantial tumor necrosis. The itemized results for each tumor specimen(by tumor radius) are tabulated in table [illegible].

Tumor Diameter(cm) (t = 6 weeks)	Tumor Diameter(cm) (t = 7 weeks)	$[(TD\ 7)^3-(TD\ 6)^3]/(TD\ 6)^3 \times 100$
Renal Adenocarcinoma		
4.5	3.8	-39.8%
4.0	3.0	-57.8%
3.5	2.9	-43.1%
3.2	2.7	-39.9%
2.6	2.0	-54.5%
2.1	1.6	-55.8%
1.5	1.0	-70.4%
1.0	0.75	-57.8%
0.75	0.50	-70.4%
0.50	0.40	-48.8%
Rhabdomyosarcoma		
2.5	2.2	-31.9%
1.6	1.2	-57.8%
1.2	1.0	-42.1%

Table 6: Pre-Treatment and Post-Treatment values for Tumor Diameter and percent change in tumor volume for both tumor systems.
Note: TD 6 = tumor diameter at 6 weeks post implantation
TD 7 = tumor diameter at 7 weeks post implantation

A unique feature of thrombin therapy is that it has two factors which work toward tumor regression; specifically internal necrosis and a systemic reduction in perfusion leading to furthur internal as well as peripheral necrosis. Traditional radio and chemo-therapies generally exert there major cell killing effect over a more focused region namely the mitotic cells of the tumor periphery leaving most of the tumor cells viable for regrowth in the future. Expressed graphically(Figure 22) the effect of thrombin therapy on the wall thickness of the proliferative tumor cell mass is to cause it to converge to zero; whereas, conventional therapies only approach a zero thickness of the proliferative tumor cell mass asymptotically due to cellular regrowth after therapy.

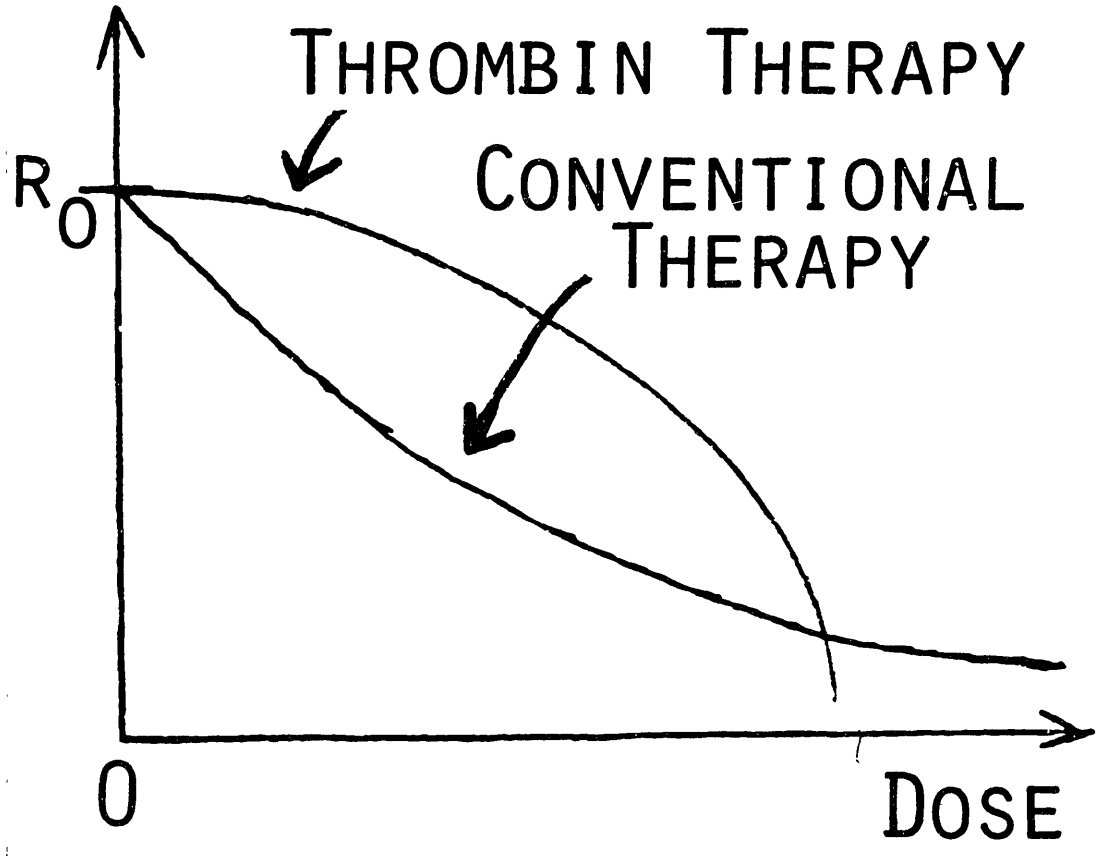

Figure 22: Qualitative representation of the thickness(r) of the proliferative tumor cell region as a function of the cumulative thrombin dose and cumulative present day chemo/radio-dose.

5. CONCLUSIONS

5.1 Tumor Vascular Morphpolgy

This examination has provided evidence that a tumor engulfs a fraction of its own vasculature as it grows. The arguments supporting this claim are:

(1) Inward radial tumor vessels exist with at least 95% certainty.

(2) Two classes of inward radial tumor vessels are found:

Class 1: Tumor vessels that show no mitotic endothelial cell impressions and are open-ended.

Class 2: Tumor vessels that show mitotic endothelial cell impressions and are closed-ended.

The existence of class 1 tumor vessels could be due to the expansion of the necrotic region of the growing tumor and the concomitant engulfment of radial tumor vessels. The local secretion of TAF to stimulate vascular sprouting from venules adjacent to the proliferating surface of the tumor results in class 2 tumor vessel formation.

Class 1 tumor vessels are present in many micrographs(e.g. Figures 15, 16) where collapsing open-ended radial tumor vessels are observed adjacent to the tumor necrotic region. The existence of these vessels could provide a pathway from the tumor interior to the main circulatory system through which detached cancer cells in the hypoxic region of the

tumor can travel. Moreover, the existence of Class 1 tumor vessels supports the hypothesis that an expanding tumor engulfs its own vasculature.

Class 2 vessels are present among the radial tumor vessels arising from sprouting vascular buds. Additionally, mitotic endothelial cells are observed at the tip and periphery of many of these vascular projections (e.g. Figures 12a, 12b, 13) indicating growth.

5.2 The Vascular Metastatic Pathway

This examination indicates that Class 1 tumor vessels provide a pathway for metastasis in the following ways:

(1) With greater then 99% confidence($p < 0.01$) there is a significant increase in the time to metastasis and concomitant decrease in the number of open-ended tumor vessels between treated and control cohorts.

(2) A greater than 95% inverse square correlation is established be tween N and t in both the treated and control cases. As a result the blockage of the tumor vascular network via the use of a direct acting coagulant inhibits metastasis.

5.3 Thrombin as an Anti-Metastatic and Tumor-Toxic Agent

Evidence suggests that thrombin therapy might be advantageous because of the synergistic reduction in the peripheral tumor volume and expansion of the tumor necrotic region which leads to an absolute convergence to zero for the radius of the proliferative tumor cell layer. Note that at one week post therapy:

(1) Renal Adenocarcinoma: 53.9 $\pm$ 0.7% reduction in tumor volume.

(2) Rhabdomyosarcoma: 43.9 $\pm$ 0.5% reduction in tumor volume.

Therefore, tumor thrombosis acts as a perfusion blocker leading to the expedient destruction of the primary tumor cells and inhibition of secondary blood-borne metastases.

For therapy of solid tumors this method has the advantage of allowing localization of the drug through the entire tumor mass at therapeutic levels while the periphery is maintained at sub-therapeutic levels. This concentration gradient is attained by calculating the dose prescribed by elementary diffusion principles(Appendix D) and then administering the bolus injection at a designated location. Also, more than 90% of malignant neoplasms are solid tumors and of those about 75% are surgically accessible by this mode of therapy.

5.4 Risks of Thrombin Therapy

The formation of pulmonary emboli could be a risk factor with the type of therapeutic protocol employed in this study. In practice, however, a complimentary systemic dose of heparin could be administered intravenously to protect against the formation of peripheral emboli should the dose of thrombin entering the tumor periphery exceed therapeutic levels. However, this is unlikely since the drug will be diluted in the total blood volume once it has exited the tumor. Finally, no problems with pulmonary emboli were encountered in 120 animals treated in this study(+ over 380 used in prior studies) and no harmful side effects of the drug were noted over the duration of the treated animal's life.

5.5 RECOMMENDATIONS

This work has provided the baseline evidence for a vascular model for metastasis. Based on this model a therapy aimed at metastatic prevention as well as tumor destruction was developed and tested in both a carcinoma and sarcoma mammalian malignancy. The results of this single dose therapy were quite successful and now furthur testing of the therapy as well as the vascular metastatic model remain to be performed in order that the therapy reach a clinical setting.

First, one needs to investigate the results of a fractionated thrombin dose study with respect to tumor death and recurrence. In this study, the delay to metastasis of the animal post treatment was increased by 100% after only a single thrombin injection to the adenocarcinoma tumor. Therefore, one would expect to be able to prevent metastasis as well as the primary tumor with a fractionated therapeutic approach.

Second, in order to establish the therapy's increased efficacy compared to conventional therapies one would conduct experiments to show that the thickness of the proliferative tumor cell layer converges to zero absolutely and not asymptotically. This can be done by histologically measuring the necrotic diameter and the tumor diameter as a function of time post thrombin treatment with a single or multiple dose protocol. The results of this experiment would quantify the effects of thrombin induced ischemia and necrosis on the primary tumor.

For multiple fraction treatments the following doses should be used:

fraction	Units/injection	Total Units
1	U(as given in equation 1)	U
2	.857 U	1.714 U
3	.833 U	2.50 U
4	.800 U	3.20 U
5	.750 U	3.75 U
6	.667 U	4.00 U

Table 7: Listing of doses used in fractionation experiment.

Three days after the administration of the final fraction of thrombin in each treatment cohort the tumor necrotic region should be injected with trypan blue, a vital stain which is exclusively absorbed by non-living cells. The tumor specimen should then be sectioned into 1 mm thick slices and placed on a 5 cm x 5 cm glass slide and mounted on a light box for viewing with a video camera. Using the image processor the image of the tumor section can be placed on a numerical grid which fixes the position of each point of the specimen in space. Using a planometer the perimeter of both the tumor's necrotic and outer border can be traced and a calculation of the enclosed cross sectional areas can be performed. These areas are stored in memory and the procedure is repeated for each

slice resulting in a three dimensional reconstruction of the solid tumor's necrotic volume and total tumor volume which can be displayed on a true three dimensional display system(Genisco Spacegraph).

Tumor specimens from each fractionated treatment cohort should be examined in a like manner at 6, 9, 12, 15, 18 and 21 days post thrombin therapy. The three dimensional volume images of the tumor's necrotic and viable tissue regions can then be displayed and compared in time post thrombin therapy. This comparison enables one to examine the efficacy of the thrombin therapy at various fractionated dose levels and to establish the best treatment plan for a tumor of a given volume. Finally, in order to establish the efficacy of the treatment on the prevention of metastasis one group of animals(15) from each treatment cohort(100 total) should be returned to their cages and maintained until expiration. The cause and time of death post tumor implantation should be recorded.

Thrombin can also be used in conjunction with other tumor therapy modalities. Thrombin therapy induces ischemia(decreased perfusion) which leads to tumor cell hypoxia and hypoxic cells have increased sensitivity to high LET radiation(e.g. neutrons, charged particles). Therefore, irradiation of the tumor with a neutron or charged particle beam after thrombin therapy will have a higher tumor cell killing effect. Also, ischemia causes a decrease in the rate of heat exchange via the tumor circulation and, as a result, heat administered to the tumor in

hyperthermia treatments would remain localized longer. Consequently, the hyerthermia therapy would have increased efficacy. In summary, thrombin therapy could have synergistic action in combination with other forms of tumor therapy. These possible effects should be investigated.

Finally, one would like to administer thrombin therapy to non-renal tumor systems, such as hepatic or pulmonary. The establishment of the therapy's efficacy in the treatment of other malignancies would support the generalizability of the method for use as a modern day method for cancer therapy.

Appendix A

Preparation of Solutions and Materials, Histological Methods

A. Dose of anethesia:

1. Inhalation: Metofane, 50 mg/kg body weight
2. Intramusclar: Sodium Pentobarbital 50 mg/kg of body weight

B. Buffered gluteraldehyde: ph=7.4, Osmolarity=320 osmols, for a final concentration of 2.5%.

$NaH_2PO_4 \cdot H_2O$	3.31 gm
$NaHPO_4 \cdot 7H_2O$	33.71 gm
25% gluteraldehyde in H_2O	40.0 ml
Distilled H_2O to make	1000.0 ml

C. Preparation of Mercox: The monomer to initiator weight ratio

Ratio = 100:1

In table A.1 is given the amount of monomer and polymer prepared for kidney-tumor systems of a given age.

Hardening Time: 20-25 minutes

System	Monomer(gm)	Initiator(gm)
Both kidneys normal(control)	8.0	0.08
4 week tumor on left kidney + normal right kidney	12.0	0.12
6 week tumor on left kidney + normal right kidney	15.0	0.15
8 week tumor on left kidney + normal right kidney	20.0	0.20

Table A.1: Listing of monomer and polymer amounts used to cast kidney-tumor systems of varying tumor ages.

Just prior to the injection of the polymer, the previously measured monomer and initiator were mixed. The mixture was drawn immediately with 10 cc syringe and injected through an 18 gauge angiocath into the perfusion line. Note that the polymer and monomer should be measured and stored in glass beakers before use because plastic materials will react with these substances at temperatures as low as $0^{o}C$.

D. KOH for digestion of cast: 20 gm of KOH pellets added to 100 ml of

distilled H_2O. Solution normality = 5.6 N.

Histological Methods

Preparation of Parrafin Sections:

1. Sierra's Fixiative (an aqueous fixiative suitable for subsequent staining with acidic and basic dyes):

95% ethanol	6 parts
Formalin	3 parts
Glacial Acetic Acid	1 part

2. Procedure:

A. Small pieces(thickness < 5 mm) of tissue are fixed from 2 to 24 hours, depending on size and nature of the tissue.

B. Dehydrate fixed tissue by rinsing in:

1. 95% ethanol --- 3 changes of 1 hour each
2. 100% ethanol -- 2 changes of 1 hour each
3. half 100% ethanol/half chloroform -- until tissue sinks(approximately one half hour).
4. chloroform ---- overnight or longer.

C. Infilitrate in 60°C oven:

1. half chloroform/half parrafin	one half hour
2. parrafin(several changes)	2 hours total

D. Embed in parafin:

1. Put together a stainless steel base and a white plastic embedding ring.
2. Nearly fill the ring with melted paraffin and immediately place tissues at bottom(using warm forceps). BE SURE no film has formed on the surface of the paraffin before tissue is inserted.
3. Holding mold by metal base, partially immerse in cold water until a film has formed on the surface of the paraffin(blowing lightly over surface is helpful).
4. When film is adequate to support water, submerge mold. Leave in cold water until paraffin block rises to the surface. (This rapid cooling prevents crystalization of paraffin).

E. Slide preparation:

1. Trim block in the form of a truncated pyramid (apex = cutting face). Sides of block faces must be parallel.
2. Section at 5-10 microns using a rotatry microtome.

3. Coat glass slides with a thin film of albumen.
4. Float sections on slides using distilled H_2O, and then heat on warming table at 45°C.
5. Allow sections to dry thoroughly before staining (usually overnight).

Hematoxylin and Eosin Stain for Paraffin Sections

A. Deparaffinize sections with xylene	7 min.
B. Hydrate in:	
1. half xylene/half 100% ethanol	2 min.
2. 100% ethanol	2 min.
3. 95% ethanol	2 min.
4. 70% ethanol	2 min.
5. 50% ethanol	2 min.
6. distilled H_2O	2 min.
C. Stain in Ehrlich's Hematoxylin	30 sec.

D. Wash in running H_2O until excess stain is no longer visible in wash water.

E. Differentiate in:

1. acid alcohol (HCL in 70% ethanol)	rinse only
2. alkaline alcohol (NH_4OH in 70% ethanol)	rinse only or until section turns blue.
3. place in 70% ethanol and examine section	

F. Eosin — 2 min.

G. Dehydrate in alcohol and clear in xylene:

1. 95% ethanol	quick rinse
2. 100% ethanol	1 min.
3. half 100% ethanol/half xylene	2 min.
4. xylene(2 changes)	7 min. total

H. Mount in Permount.

I. If necessary, excess eosin may be removed by soaking off coverslip in xylene and returning through 100% ethanol to a quick rinse in 95% ethanol, then dehydrating and clearing as in Steps 1-4(G).

Eosin Stain

Stock Solution:	Eosin Y	1 gm
	70% ethyl alcohol	1000 ml
	Glacial Acetic Acid	5 ml

Working Solution: Dilute stock solution with an equal volume of 70% alcohol and add 2-3 drops of acetic acid(stock).

Appendix B

List of Materials and their Manufacturing Companies

Ammonium Hydroxide: Stock

Fisher Scientific Co., Fair Lawn, N.J. 07410

Aluminum Stubs: 15 mm diameter, 10 mm high

Research Ind., Inc., Burlington, Vermont 05401

Angiocath: 18 gauge, 1.5 inch

Desert Co., Sandy Utah 84070

Autoclips: 9 mm, non-sterile

Clay Adams, Parsippany, N.J. 07054

Chloroform: Stock

Fisher Scientific Co., Fair Lawn, N.J. 07410

Copper grids: Carbon stabilized

Ted Paella, Tustin, Ca. 92680

Ehrlich's Hemotoxylin: Stock

Fisher Scientific Co., Fair Lawn, N.J. 07410

Eosin Y: Stock

Fisher Scientific Co., Fair Lawn, N.J. 07410

Ethanol: Pure ethyl alcohol, dehydrated

U.S. Industrial Chemical, N.Y., N.Y.

Formaldehyde: Stock

Fisher Scientific Co., Fair Lawn, N.J. 07410

Glacial Acetic Acid: Stock

Fisher Scientific Co., Fair Lawn, N.J. 07410

Gluteraldehyde: 25% in H_2O, Practical grade

J.T. Baker Chemical Co., Phillipsburg, N.J. 08865

Heparine: Heparine Sodium, Lab grade

Fisher Scientific Co., Fair Lawn, N.J. 07410

Hydrochloric Acid: Stock

Fisher Scientific Co., Fair Lawn, N.J. 07410

Light Microscope: Zeiss Model# 47 79 01 9901

D-7082 Oberkochen, West Germany

Metofane: 50 mg/cc; Inhalation Anesthetic

Pitman-Moore, Inc., Washington Crossing, N.J. 08560

Mercox: Blue(Methyl Methacrylate)

Ladd Research Industries, Inc., Burlington, Vermont 05401

Parrafin: Solid(White)

Fisher Scientific Co., Fair Lawn, N.J. 07410

Pottasium Hydroxide: Dry solid pellets

MCB Manuf., Cincinnati, Ohio 45212

Rat: Wistar-Lewis, Female, 300 gms.

Charles River Co., Ma. 02139

Rat: Wag-Rij, Female, 200 gms.

Lawrence Berkeley Laboratory, Berkeley, Ca. 94720

Renal adenocarcinoma: Tumor System

Dr. Richard Babayan, Boston City Hospital, Boston, Ma.

Dr. Alan C. Nelson, MIT Cambridge, Ma.

Rhabdomyosarcoma: Tumor System

Dr. Stan Curtis, Lawrence Berkeley Laboratory, Berkeley, Ca. 94720

RPMI growth medium: #1640, with 25 mM Hepes

M.A. Bioproducts, Walkersville, Maryland 21793

Saline: 0.85%, Sterile, physiological pH

Fisher Scientific Co., Fair Lawn, N.J. 07410

Scanning Electron Microscope: DS-130

ISI, Mountain View, Ca.

Silver colloid:

Ted Pella Inc., Tustin, CA. 92680

Sodium Pentobarbital: Anesthetic

Pitman-Moore, Inc., Washington Crossing, NJ 08560

Sodium Phosphate: Dibasic, Heptahydrate

Fisher Scientific Co., Fair Lawn, NJ 07410

Sodium Phosphate: Monobasic, Crystals

MCB Manufactor, Cincinnati, Ohio 45212

Sputter Coater: SEM coating unit E51000

Polaron Instruments Inc.

Sutures: Dexon 3-0

Davis-Geck, P.R. 00701

Thrombin: USP Bovine origin

Parke-Davis, Morris Plains, NJ 07950

Water: Distilled

Fisher Scientific Co., Fair Lawn, NJ 07410

Xylene: Stock

Fisher Scientific Co., Fair Lawn, NJ 07410

Appendix C

The Structure and Physiological Role of Thrombin:

Thrombin is a multifunctional enzyme, which may react specifically with several proteins and cells(via receptors) as well as nonspecifically with the surfaces(e.g. mucopolysaccharides) or with other molecules(Machovich, 1981; Fenton, 1981). Its main targets are summarized in figure C.1.

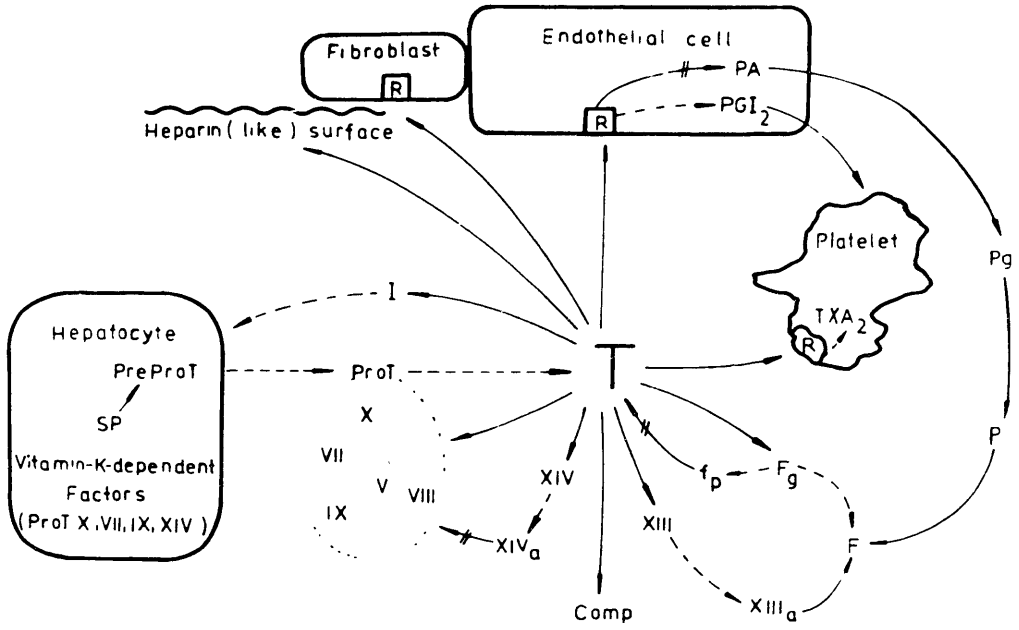

FIGURE 1 Biological functions of thrombin Roman numerals stand for blood coagulation factors, dotted line for activation complex, solid arrows for interaction of thrombin with various components, dashed arrows for conversion and crossed arrows for inhibition. Other abbreviations PreProT = preprothrombin, SP = signal peptidase, ProT = prothrombin, T = thrombin, I = inhibitor (antithrombin III, α-2-macroglobulin, α-1-proteinase inhibitor), R = receptor, Comp = complement component proteins, PGI_2 = prostacyclin, PA = plasminogen activator, Pg = plasminogen, P = plasmin, F = fibrin, Fg = fibrinogen, fp = fibrinopeptides

Figure C.1: Biological functions of thrombin.

The function of thrombin in the maintenance of hemostatic balance is attained by several biological reactions. According to modern day knowledge, its main function is the catalysis of the fibrinogen-fibrin conversion. The fibrin thrombus formed, however, is not the final form of a thrombus. In nearly all cases, aggregates of platlets are found in the thrombus. Furthermore, the size and stability of the clot is further modified by another enzyme, Factor XIIIa. Thrombin plays a major role in above-mentioned two processes as well: its binding to platlets initiates changes in the cell metabolism and its reaction with Factor XIII results in the activation of the proenzyme, fibrinogen.

In addition, thrombin binds to endothelial cells with high affinity, inducing prostacyclin release and several other biochemical reactions. Thrombin regulates its own concentration through reactions with prothrombin, Factor V, Factor VII, and Protein C. Besides these, more than ten other biological functions of thrombin are known, although their importance in the maintenance of hemostatic balance, is under investigation.

Thrombin is a highly specific proteolytic enzyme. It is a serine protease with trypsin-like specificity. The primary structures of the bovine and human enzymes have been determined(Blomback, 1969; Iwanaga, 1964) and are shown in figure C.2. The active site residues actually

serine(#205). These three residues interact during the process of catalysis.

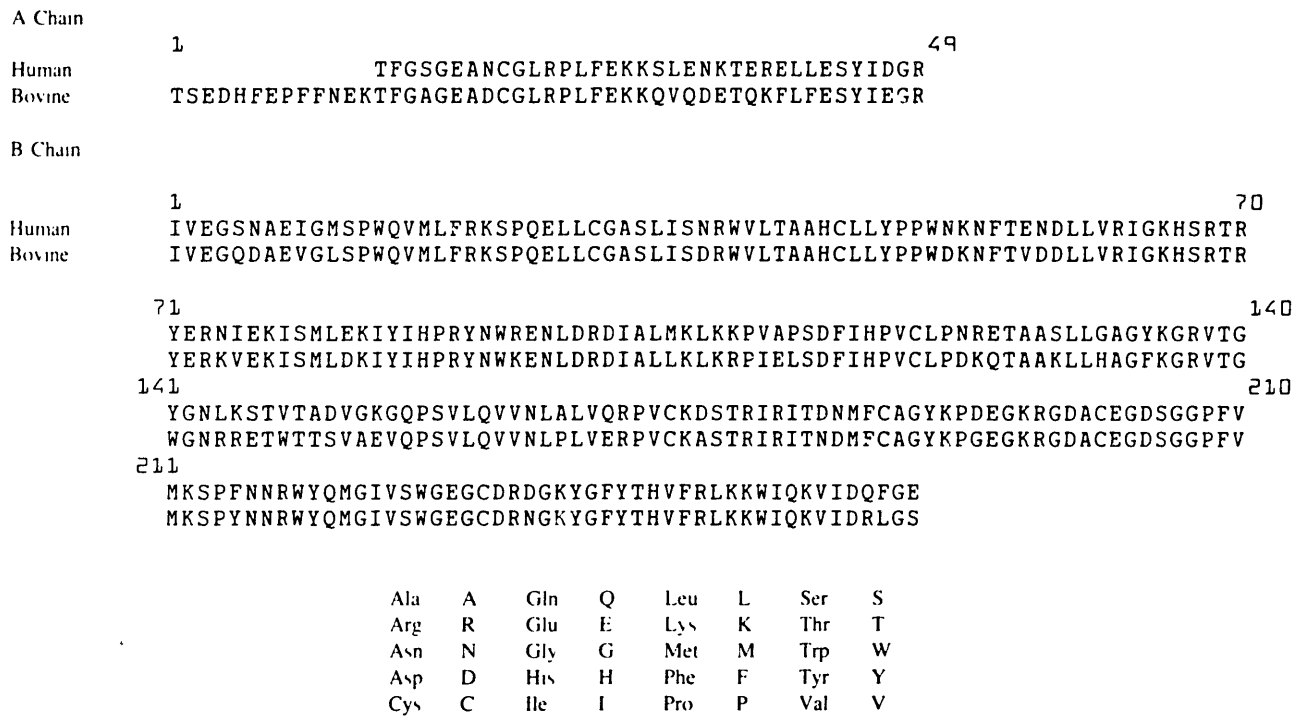

Ala	A	Gln	Q	Leu	L	Ser	S
Arg	R	Glu	E	Lys	K	Thr	T
Asn	N	Gly	G	Met	M	Trp	W
Asp	D	His	H	Phe	F	Tyr	Y
Cys	C	Ile	I	Pro	P	Val	V

Figure C.2: Structure of human and bovine alpha thrombin.

Appendix D

Thrombin Dose Calculation

The thrombin dose administered is a function of tumor radius and has been calculated. It is assumed that the injected dose of thrombin diffuses isotropically through tissue and can be modeled as an instantaneous point source. Under these conditions the concentration of thrombin as a function of radius(r) and time(t) is given by the solution to the time dependent diffusion equation:

$$\nabla^2 C(r,t) = (D)^{-1} dC(r,t)/dt \qquad (D.1)$$

where:

r = radius in cm (point of injection[r=0])

t = time in sec (time of injection, $t_0 = 0$)

D = 1.8 E-5 cm^2/sec

(thrombin diffusion coefficient in tissue),(Choi,1961)

The thrombin injection initially occupies a small volume of radius, a, whose concentration is given by:

$$C(r,t) = C_0 \quad \text{for } 0 < r < a$$

$$C(r,t) = 0 \quad \text{for } r > a$$

Using these boundary conditions we find the solution to equation (D.1):

$$C(r,t) = [U/8(\pi Dt)^{1.5}e\{-r^2/4Dt(1+(r^2/Dt-6)a^2/40Dt\}] \quad (D.2)$$

where $U = 4/3\pi a^3 C_o$

In the limit as a approaches zero and U is kept constant(i.e C_o increases), equation(D.2) reduces to a point source function:

$$C(r,t) = (U/8(\pi Dt)^{1.5})e^{(-r^2/4Dt)} \quad (D.3)$$

Rearranging,

$$U = C(r,t)8(\pi Dt)^{1.5}\ e^{(r^2/4Dt)} \quad (D.4)$$

At $t = t_{max} = r^2/6D$ and $C(r,t) = C_{therapeutic}(r,t) = 2$ units/ml

equation D.4 becomes:

$$U = C_{therapeutic}(r,t)8(\pi er^2)^{1.5} \quad (D.5)$$

or

$$^{*}U = 8(2 \text{ units/ml}) \cdot (\pi er^2)^{1.5} \qquad (D.6)$$

* Note: The value of U calculated by equation D.6 will overestimate the actual value by the fraction (Tumor volume/Vascular volume) because the calculation above derives a value for U based on the assumption that the drug is diffusing through a sphere of blood; whereas the tumor tissue is comprised of cells, blood, connective tissues, and air space.

Therefore the most accurate value for U is given by:

$$U' = 8(2 \text{ units/ml}) \cdot (\pi er^2)^{1.5} \text{ (vascular volume}/1.333r^3)$$

```
c     ------------------------------------------------------------
c                        Thrombin Dose Calculation
c                           Computer Routine
c     ------------------------------------------------------------
c
c     This routine is designed to calculate the number of units
c     thrombin one should administer to the tumor necrotic region
c     such that at time, tmax the dose of thrombin will have reached
c     therapeutic levels throughout the entire tumor mass.
c
c     ------------------------------------------------------------

      real*4 re, units, tmax, vv
      alpha = 399.3
      beta = .3888
      print *, ' '
      print *, 'Enter tumor radius(in cm): '
      print *, ' '
      Accept 10, re
10    format(f10.4)
      print *, ' '
      print *, 'Enter vascular volume(in ml): '
      print*, ' '
```

```
      Accept 20, vv
20    format(f10.4)
      units = (alpha) * (vv/(1.333*re**3)) * re**3
      print *, ' The number of thrombin units needed = ', units
      tmax = (re**2)/beta
      print *, 'tmax = ', tmax
      stop
      end
```

REFERENCES

Babayan, R., Nelson, A.C., and Shah, A.(1984), "Polymer casting technique for the study of normal and abnormal renal vasculature," American Urological Association, Proceedings of the 1983 annual meeting, K-27.

Babayan, R., Nelson, A.C., and D'Amico, A.V.(1985), "A novel approach to the study of microvasculature in solid tumors", American College of Surgeons 1985 Surgical Forum Volume XXXVI.

Barendsen, G.W., Broerse, J.J.,(1970), European J. Cancer, Vol. 15, p. 373-385.

Bevington, P.R.,(1969), Data Reduction and Error Analysis for the Physical Sciences, McGraw Hill Book Company, pp. 50-125, New York, New York.

Blomback, B.,(1969), "The N-terminal disulfide knot of human fibrinogen", British Journal of Hematology, Vol. 17, pg. 145-166.

Chew, E.C., Wallace, A.C.,(1976), "Demonstration of fibrin in early stages of experimental metastases," Cancer Research, V. 36, p. 1904-1917.

Choi,H., Rosenhow, F.,(1961),"Heat, Mass, and Momentum Transfer," edited by Krwadleigh and J. B. Reswick, Prentice Hall International Series in Engineering, pp. 503-529.

D'Amico, A.V.,(1985), "The use of solid tumor microvasulature studies to investigate the metastatic process," Proceedings of the 1985 Radiation Reseach meeting, HI-9.

D'Amico, A.V.,(1986), "Thrombin: Potential uses in Cancer Therapy", Proceedings of the 1986 Radiation Research meeting, Fh-16.

Duncan, R.C., Knapp, R.G., Miller, M.C. III,(1977), Introductory Biostatistics for the Health Sciences, Second edition, John Wiley and Sons, New York, pp. 198-199.

Dvorak, H.F., et al.,(1979), "Induction of a fibrin gel investment: An early event in line 10 hepatocarcinoma growth mediated by tumor secreted products," J. Immunology, V. 122, p. 166-187.

Fenton, J.W.,II,(1981), "Thrombin Specificity", Ann. N.Y. Acad. Sci., Vol. 370, pg. 468-489.

Folkman, J., Cotran, R.S.(1976), International Review of Experimental Pathology, G.W. Richter, ed. pp. 207-298.

Folkman, J. and Tyler, K.(1975),"Tumor Angiogenesis: Its role in metastasis and invasion," in Cancer: A Comprehensive Treatise, Vol. 3, ed. by F.F. Becker, Plenum Press, New York, pp. 355-388.

Folkman, J.(1985), "Tumor Angiogenesis," Adv. Cancer Research, Vol. 43, pp. 175-203.

Iwanaga, S., Wallen, P., Gradahl, N.Y., Henschen, A., and Blomback, B.(1964), "On the primary structure of human fibrinogen. Isolation and characterization of N-terminal fragments from plastic digests", European Journal of Biochemistry, Vol. 8, pg. 189-201.

Kallmann, R.F.(1972), "The phenomenon of reoxygenation and its implications for fractionated radiotherapy," Radiology, Vol. 105, pp. 135-142.

Kramer, R.H., Nicolson, G.L.(1979), "Interactions of tumor cells with vascular endothelial cell monolayers: A model for metastatic invasion", Proc. Natl. Acad. Sci., U.S.A. V. 76, p. 5704-5712.

Langer, R., Folkman, J.(1976), Nature, V. 263, pp. 797-800.

Liotta, A., Kleinerman, J. and Saidel, G.M.(1974) "Quantitative relationships of intravascular tumor cells, and pulmonary metastases following tumor implantation," Cancer Research, Vol. 34, pp. 997-1004.

Machovich, R. and Horvath, I.(1981), "Thrombin and haemostasis: regulation of the biological functions of thrombin, Haematologia, Vol. 14, pg. 339-356.

Nelson, A.C., Shah-Yukich, A., and Babayan, R.(1984) "Radiation damage in rat kidney microvasculature," SEM/1984, pp. 4214-4219.

Nicolson, Garth L.(1979)," Cancer Metastasis," Scientific American, Vol. 240, No. 3, pp. 66-93.

Peterson, H.I.(1979), Tumor Blood Circulation, CRC Press, Florida, pp. 1-43, and 144-164.

Poste, G.(1977),"The cell surface and metastasis," in Fundamental Aspects of Metastasis, Chapter 2, by Leonard Weiss, pp. 25-45.

Salsbury, A.J. and Griffiths, J.D.(1965), "The Fate of Circulating Cancer Cells," Circulating Cancer Cells, ed. I. Newton Kugelmass, Charles C. Thomas Publisher, Illinois, pp. 100-134.

Shah, A. (1983) "A three dimensional characterization of solid tumor microvasculature," Ph.D. Thesis, Massachusetts Institute of Technology, Department of Nuclear Engineering, Cambridge, Massachusetts.

Turner, G.A. and Weiss L. (1980), "Some effects of products from necrotic regions of tumors on the in vitro migration of cancer and peritoneal exudate cells," Int. J. Cancer, Vol. 26, pp. 247-254.

Weiss, L.(1978), "Some mechanisms involved in cancer cell detachment by necrotic material," Int. J. Cancer, Vol. 22, pp. 196-203.

White, R.D. and Olsson, C.G.(1980), "Renal Adenocarcinoma in the rat: A new tumor model," Investigative Urology, Vol. 17, No. 5, pp. 405-412.